blood®
Regular Article

Check for updates

MYELOID NEOPLASIA

Germ line variant GFI1-36N affects DNA repair and sensitizes AML cells to DNA damage and repair therapy

Daria Frank,[1,2] Pradeep Kumar Patnana,[1-3] Jan Vorwerk,[1] Lianghao Mao,[4] Lavanya Mokada Gopal,[4] Noelle Jung,[4] Thorben Hennig,[4] Leo Ruhnke,[5] Joris Maximillian Frenz,[4] Maithreyan Kuppusamy,[4] Robert Autry,[6] Lanying Wei,[1,7] Kaiyan Sun,[1] Helal Mohammed Mohammed Ahmed,[1,3] Axel Künstner,[8,9] Hauke Busch,[8,9] Heiko Müller,[10] Stephan Hutter,[10] Gregor Hoermann,[10] Longlong Liu,[1,11] Xiaoqing Xie,[1,12] Yahya Al-Matary,[13] Subbaiah Chary Nimmagadda,[1,3] Fiorella Charles Cano,[14] Michael Heuser,[14] Felicitas Thol,[14] Gudrun Göhring,[15] Doris Steinemann,[15] Jürgen Thomale,[16] Theo Leitner,[3] Anja Fischer,[17,18] Roland Rad,[17-19] Christoph Röllig,[6] Heidi Altmann,[6] Desiree Kunadt,[6] Wolfgang E. Berdel,[1] Jana Hüve,[20] Felix Neumann,[20,21] Jürgen Klingauf,[20,22] Virginie Calderon,[23] Bertram Opalka,[2] Ulrich Dührsen,[2] Frank Rosenbauer,[24] Martin Dugas,[25] Julian Varghese,[7] Hans Christian Reinhardt,[2] Nikolas von Bubnoff,[3] Tarik Möröy,[26-28] Georg Lenz,[1] Aarif M. N. Batcha,[29,30] Marianna Giorgi,[31] Murugan Selvam,[31] Eunice Wang,[31] Shannon K. McWeeney,[32-34] Jeffrey W. Tyner,[33,35] Friedrich Stölzel,[5,36] Matthias Mann,[37] Ashok Kumar Jayavelu,[4,6,37,38] and Cyrus Khandanpour[1-3]

[1]Department of Medicine A, Hematology, Oncology and Pneumology, University Hospital Münster, Münster, Germany; [2]Department of Hematology and Stem Cell Transplantation, University Hospital Essen, Essen, Germany; [3]Department of Hematology and Oncology, University Hospital of Schleswig-Holstein, University Cancer Center Schleswig-Holstein, University of Lübeck, Lübeck, Germany; [4]Proteomics and Cancer Cell Signaling Group, Clinical Cooperation Unit Pediatric Leukemia, German Cancer Research Center and Department of Pediatric Oncology, Hematology and Immunology, University of Heidelberg, Heidelberg, Germany; [5]Department of Internal Medicine I, University Hospital Dresden, Technical University Dresden, Dresden, Germany; [6]Hopp Children's Cancer Center, Heidelberg, Germany; [7]Institute of Medical Informatics, University of Münster, Münster, Germany; [8]Medical Systems Biology Group, Lübeck Institute of Experimental Dermatology, and [9]Institute for Cardiogenetics, University of Lübeck, Lübeck, Germany; [10]MLL Munich Leukemia Laboratory, Munich, Germany; [11]Department of Hematology, First Affiliated Hospital, Guangzhou Medical University, Guangzhou, China; [12]Department of Hematology-Oncology, Chongqing University Cancer Hospital, Chongqing, China; [13]Department of Dermatology, University Hospital Essen, Essen, Germany; [14]Department of Hematology, Hemostasis, Oncology and Stem Cell Transplantation, and [15]Department of Human Genetics, Hannover Medical School, Hannover, Germany; [16]Institute of Cell Biology, University Hospital Essen, Essen, Germany; [17]Institute of Molecular Oncology and Functional Genomics, [18]Center for Translational Cancer Research, and [19]Department of Medicine II, Klinikum Rechts der Isar, School of Medicine, Technische Universität München, Munich, Germany; [20]Fluorescence Microscopy Facility Münster, Institute of Medical Physics and Biophysics, University of Münster, Münster, Germany; [21]Refined Laser Systems GmbH, Münster, Germany; [22]Institute of Medical Physics and Biophysics, University of Münster, Münster, Germany; [23]Bioinformatic Core Facility, Institut de Recherches Cliniques de Montréal, Montréal, QC, Canada; [24]Institute of Molecular Tumor Biology, Faculty of Medicine, University of Münster, Münster, Germany; [25]Institute of Medical Informatics, University Hospital Heidelberg, Heidelberg, Germany; [26]Institut de Recherches Cliniques de Montréal, Montreal, QC, Canada; [27]Division of Experimental Medicine, McGill University, Montreal, QC, Canada; [28]Département de Microbiologie, Infectiologie et Immunologie, Université de Montréal, Montreal, QC, Canada; [29]Institute of Medical Data Processing, Biometrics and Epidemiology, Faculty of Medicine, and [30]Data Integration for Future Medicine, Ludwig Maximilian University Munich, Munich, Germany; [31]Roswell Park Comprehensive Cancer Center, Jacobs School of Medicine and Biomedical Sciences, Buffalo, NY; [32]Division of Bioinformatics and Computational Biology, Department of Medical Informatics and Clinical Epidemiology, [33]Knight Cancer Institute, [34]Oregon Clinical and Translational Research Institute, and [35]Department of Cell, Developmental and Cancer Biology, Oregon Health & Science University, Portland, OR; [36]Department of Medicine II, Division for Stem Cell Transplantation and Cellular Immunotherapy, University Cancer Center Schleswig-Holstein, University Hospital Schleswig-Holstein Kiel, Christian Albrecht University Kiel, Kiel, Germany; [37]Department of Proteomics and Signal Transduction, Max Planck Institute of Biochemistry, Munich, Germany; and [38]Molecular Medicine Partnership Unit, European Molecular Biology Laboratory and Medical Faculty, University of Heidelberg, Heidelberg, Germany

KEY POINTS

- **Presence of GFI1-36N impedes HR- and MGMT-mediated DNA repair selectively in AML cells.**
- **Use of temozolomide and olaparib allows for selective targeting of *GFI1-36N* leukemic cells.**

Growth factor independence 1 (GFI1) is a DNA-binding transcription factor and a key regulator of hematopoiesis. *GFI1-36N* is a germ line variant, causing a change of serine (S) to asparagine (N) at position 36. We previously reported that the *GFI1-36N* allele has a prevalence of 10% to 15% among patients with acute myeloid leukemia (AML) and 5% to 7% among healthy Caucasians and promotes the development of this disease. Using a multiomics approach, we show here that *GFI1-36N* expression is associated with increased frequencies of chromosomal aberrations, mutational burden, and mutational signatures in both murine and human AML and impedes homologous recombination (HR)–directed DNA repair in leukemic cells. *GFI1-36N* exhibits impaired binding to N-Myc downstream-regulated gene 1 (*Ndrg1*) regulatory elements, causing decreased NDRG1 levels, which leads to a reduction of O^6-methylguanine-DNA-methyltransferase (MGMT) expression levels, as illustrated by both transcriptome and proteome analyses. Targeting MGMT via temozolomide, a DNA alkylating drug, and HR via olaparib, a poly-ADP ribose polymerase 1 inhibitor, caused synthetic lethality in human and murine AML samples expressing *GFI1-36N*, whereas the effects were

Downloaded from http://ashpublications.net/blood/article-pdf/142/25/2175/2177539/blood_bld-2022-015752-main.pdf by guest on 03 May 2024

insignificant in nonmalignant *GFI1-36S* or *GFI1-36N* cells. In addition, mice that received transplantation with *GFI1-36N* leukemic cells treated with a combination of temozolomide and olaparib had significantly longer AML-free survival than mice that received transplantation with *GFI1-36S* leukemic cells. This suggests that reduced MGMT expression leaves *GFI1-36N* leukemic cells particularly vulnerable to DNA damage initiating chemotherapeutics. Our data provide critical insights into novel options to treat patients with AML carrying the *GFI1-36N* variant.

Introduction

GFI1 transcriptionally regulates the development of hematopoietic, neuronal, and intestinal epithelial cells.[1-5] A variant of GFI1 denominated *GFI1-36N* and characterized by an exchange of serine (S) to asparagine (N) at position 36 has a prevalence of 5% to 7% in different healthy control populations. The prevalence of the *GFI1-36N* allele is increased (10%-15%) among patients with MDS, acute myeloid leukemia (AML), and multiple myeloma, and the presence of the *GFI1-36N* allele is associated with a poor prognosis.[6-8] *GFI1-36N* leukemic cells feature increased H3K9 acetylation at target genes, resulting in higher expression of genes such as *Hoxa9*, *Pbx1*, *Meis1*, *CSF1*, and *CSFR1*,[9] driving cell survival and proliferation.[10-16] GFI1 also regulates apoptosis through regulating the methylation status of p53 in lymphoblastic leukemia[17] and MRE11 and 53BP1 in DNA repair.[18] However, it is not known how these nontranscriptional activities are affected in the *GFI1-36N* variant.

We leveraged multiomics profiling to gain mechanistic insights into the molecular architecture that drives myeloid leukemia in the presence of *GFI1-36N*. *GFI1-36N* interferes with DNA repair in leukemic cells and sensitizes malignant cells to treatment with olaparib and temozolomide, opening a new therapeutic approach to treat AML/MDS.

Materials and methods

Patient cohort

Patients with AML treated in Essen, Hannover, and Dresden (Study Alliance Leukemia AML registry biobank [IRB no. EK98032010]) as well as the MLL cohort were described previously.[6,19-22] All experiments with human samples were carried out in accordance with the approved protocol of the respective competent authority. All the patients provided written informed consent and performed according to the Declaration of Helsinki.

Mouse strains and approval

Mice carrying either the *GFI1-36N* or *GFI1-36S* allele were generated as described previously.[17] NUP98-HOXD13 transgenic mice were obtained from The Jackson Laboratory (Bar Harbor, ME).[9,22] PiggyBac Transposon mouse models were donated by the Trust Sanger Institute, Hinxton-Cambridge.[23,24] All mice were kept under specific-pathogen-free conditions, and all animal experiments were approved by the respective animal ethics committee (North Rhine-Westphalia: 84-02.04.2015.A076, 81-02.04.2019.A440 or Regierungsbezirk Oberbayern: 55.2Vet-2532.Vet_03-16-56).

Generation of leukemic cells

Lineage-negative (Lin^-) cells were isolated from the total bone marrow (BM) of knockin mice carrying either human *GFI1-36N* or human *GFI1-36S* using the Lineage Cell Depletion Kit (Miltenyi Biotec, catalog no. 130-090-858 and catalog no. 130-042-401). Lin^- cells were then cultured in IMDM media containing 20% fetal bovine serum, 1% penicillin/streptomycyn, 10 ng/ml murine interleukin-3 (mIL-3), 10 ng/mL mIL-6, and 20 ng/ml murine stem cell factor (Miltenyi Biotec, catalog no. 130-101-741, catalog no. 130-096-687, and catalog no. 130-094-065) for expansion. Lin^- cells were then transduced retrovirally with the MSCV (murine stem cell virus)-MLL (mixed lineage leukemia)-AF9-IRES (internal ribosomal entry site)–green fluorescent protein (GFP) (*MLL-AF9*; kindly provided by Jay Hess) plasmid[9,25] expressing GFP. A total of 1×10^5 positive transduced (GFP^+) Lin^- cells were transplanted IV together with 1×10^5 competitive BM cells into lethal (7 + 3 Gy)-irradiated C57BL/6 mice. Leukemic BM cells corresponding to 1×10^5 GFP^+ cells were retransplanted IV into sublethal irradiated C57BL/6 mice (3 Gy), as previously described.[9,25]

Label-free proteome quantification

Fluorescence activated cell–sorted *GFI1-36N* or *GFI1-36S MLL-AF9*–expressing leukemic cells (0.5-1 $\times 10^6$ cells per sample) from the mouse BM were thoroughly washed in plain phosphate buffered saline (PBS), lysed in 1% sodium deoxycholate (SDC) buffer (1% SDC, 100 mM Tris pH8.5, 40 mM 2-chloroacetamide, and 10 mM tris(2-carboxyethyl)phosphine), incubated on ice for 20 minutes, boiled at 95°C, and sonicated for 5 minutes on a Biorupter plus, as described previously.[26] Samples were digested with the proteases LysC (1:100 ratio) for 2 hours, followed by trypsin (1:100 ratio) overnight at 37°C. To the digested peptide volume, 5 times the volume of isopropanol/1% trifluoroacetic acid (TFA) was added and vortexed to stop the digestion. The peptides were desalted on equilibrated styrenedivinylbenzene-reversed phase sulfonated StageTips, washed once in isopropanol/1% TFA and twice with 0.2% TFA. Purified peptides were eluted with 60 µL of elution buffer (80% acetonitrile and 1.25% NH_4OH). The dried elutes were resuspended in MS loading buffer (3% ACN, 0.3% TFA) and stored at −20°C until MS measurement. For liquid chromatography mass spectrometry (LC-MS/MS) measurement, we used 200 ng peptide (concentration determined by nanodrop) per sample. Further details can be found in supplemental Methods, available on the *Blood* website. For samples from patients with AML, mononuclear cells were ficoll-enriched, washed twice in PBS, lysed, and processed as mentioned earlier.

In vitro and in vivo treatment of primary cells with temozolomide and olaparib

Temozolomide (Sigma) and olaparib (Selleckchem or MedChemExpress or AstraZeneca) were dissolved in dimethyl sulfoxide (39 mg/ml and 86 mg/mL, respectively). For the colony-forming unit assays, 0.5×10^3 to 1×10^4 primary murine cells were plated in 1 mL MethoCult media (M3434, Stemcell) and 0.5×10^3 primary

Downloaded from http://ashpublications.net/blood/article-pdf/142/25/2175/2177539/blood_bld-2022-015752-main.pdf by guest on 03 May 2024

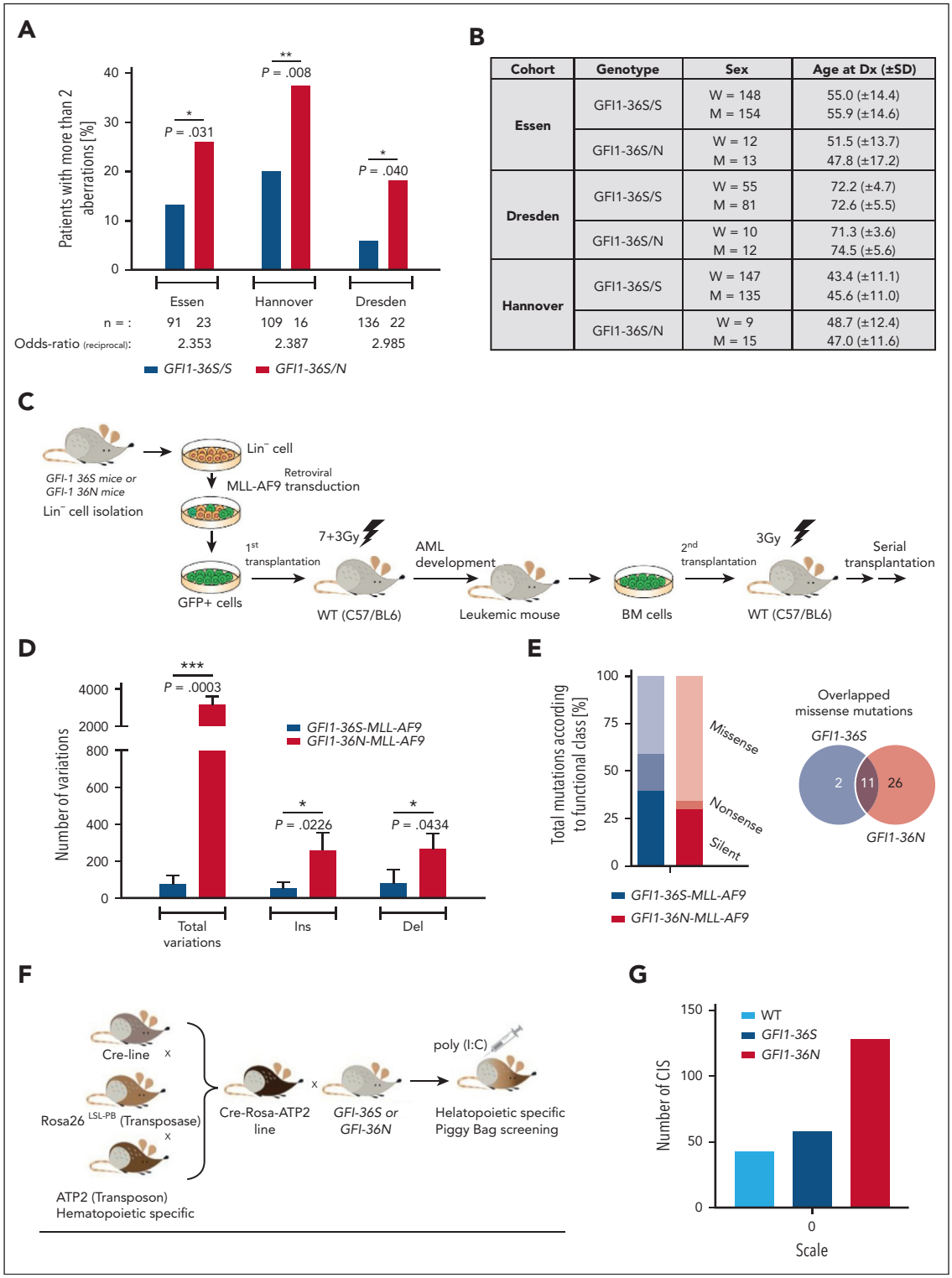

Cohort	Genotype	Sex	Age at Dx (±SD)
Essen	GFI1-36S/S	W = 148 M = 154	55.0 (±14.4) 55.9 (±14.6)
	GFI1-36S/N	W = 12 M = 13	51.5 (±13.7) 47.8 (±17.2)
Dresden	GFI1-36S/S	W = 55 M = 81	72.2 (±4.7) 72.6 (±5.5)
	GFI1-36S/N	W = 10 M = 12	71.3 (±3.6) 74.5 (±5.6)
Hannover	GFI1-36S/S	W = 147 M = 135	43.4 (±11.1) 45.6 (±11.0)
	GFI1-36S/N	W = 9 M = 15	48.7 (±12.4) 47.0 (±11.6)

Figure 1. More genetic aberrations in human and murine *GFI1-36N* AML samples. (A) Percentage of patients with MDS/AML of 3 different cohorts with >2 chromosomal aberrations. Patient samples were genotyped for the presence of *GFI1-36N* or *GFI1-36S* with real time (RT)-PCR. (B) Number of patients in individual cohorts corelating to gender and age of the patients. (C) Schematic experimental setup to generate leukemic mice and the serial transplantation experiments. (D) Serial transplanted BM cells from leukemic *MLL-AF9* mice and nonleukemic Lin⁻ cells were analyzed using RNA-seq followed by variant calling analysis. Shown is the number of variations in leukemic cells minus the number of variations in nonleukemic cells. n = 3; mean ± standard deviation. (E) Variations from (D) divided according to the functional class of mutation. Shown is the total number of mutations per genotype (left). The Venn diagram (right) represents the overlaps of missense mutations between *GFI1-36S* and *GFI1-36N* leukemic cells. (F) Scheme of the PiggyBac transposon-based mouse model. GFI1-36S or GFI1-36N mice were crossed with the PiggyBac transposon mice (Mx-Cre × Rosa26 × ATP2). Mice were injected with poly(I:C) to activate the transposon system. (G) The PiggyBac transposon-based mouse model was used to check the number of common insertion sites (CISs) of the transposon sequence. The number of CISs were calculated for each genotype. WT: n = 4, *GFI1-36S* (heterozygous [n = 6] and homozygous [n = 1]): n = 7, and *GFI1-36N* (heterozygous [n = 2] and homozygous [n = 7]): n = 9. *$P < .05$; **$P < .01$; ***$P < .001$. M, men; W, women; WT, wild-type.

Downloaded from http://ashpublications.net/blood/article-pdf/142/25/2175/2177539/blood_bld-2022-015752-main.pdf by guest on 03 May 2024

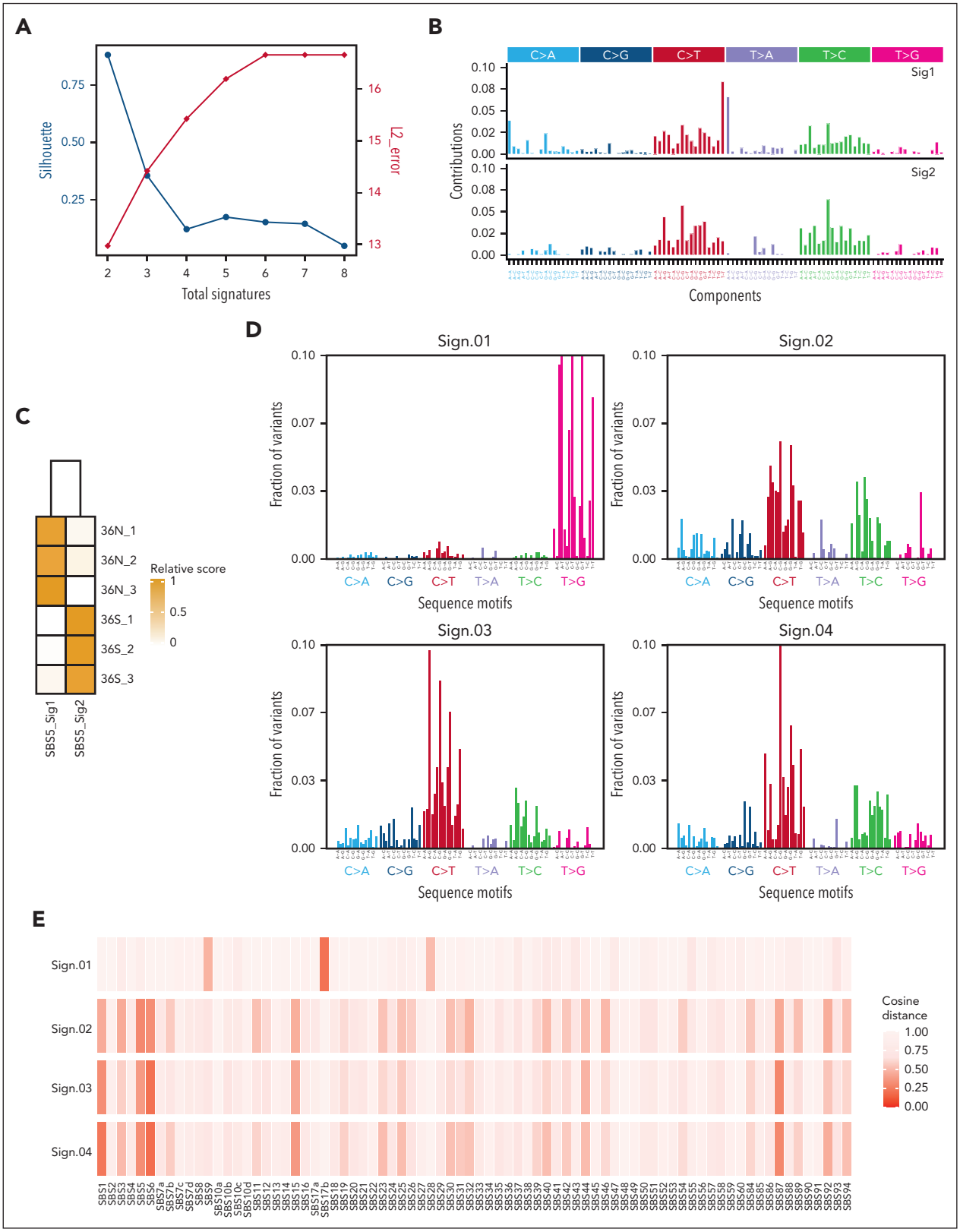

Figure 2. Somatic signatures in *GFI1-36S* and *-36N* leukemic mice and de novo identification of mutational signatures in human *GFI1-36N*–mutated samples. (A-C) RNA-seq data of BM cells from leukemic *GFI1-36S* (n = 3) and *GFI1-36S* (n = 3) mice were analyzed regarding their somatic signatures. (A) The optimal number of signatures is estimated based on silhouette coefficient (black) and L2 error (red). (B) SBS profiles considering the mutated base but also the bases immediately 5′ and 3′ for each signature and (C) signature activities for each sample. (D-E) Human *GFI1-36S* (n = 1348) and *GFI1-36N* (n = 182) samples were analyzed for their mutational signatures. (D) Mutational signatures identified in somatically enriched set of variants occurring in coding regions of clinical samples harboring *GFI1-36N*. (E) Cosine similarity of signatures Sign.01 to Sign.04 to the COSMIC single-base substitution reference set of mutational signatures version 3.3.

Downloaded from http://ashpublications.net/blood/article-pdf/142/25/2175/2177539/blood_bld-2022-015752-main.pdf by guest on 03 May 2024

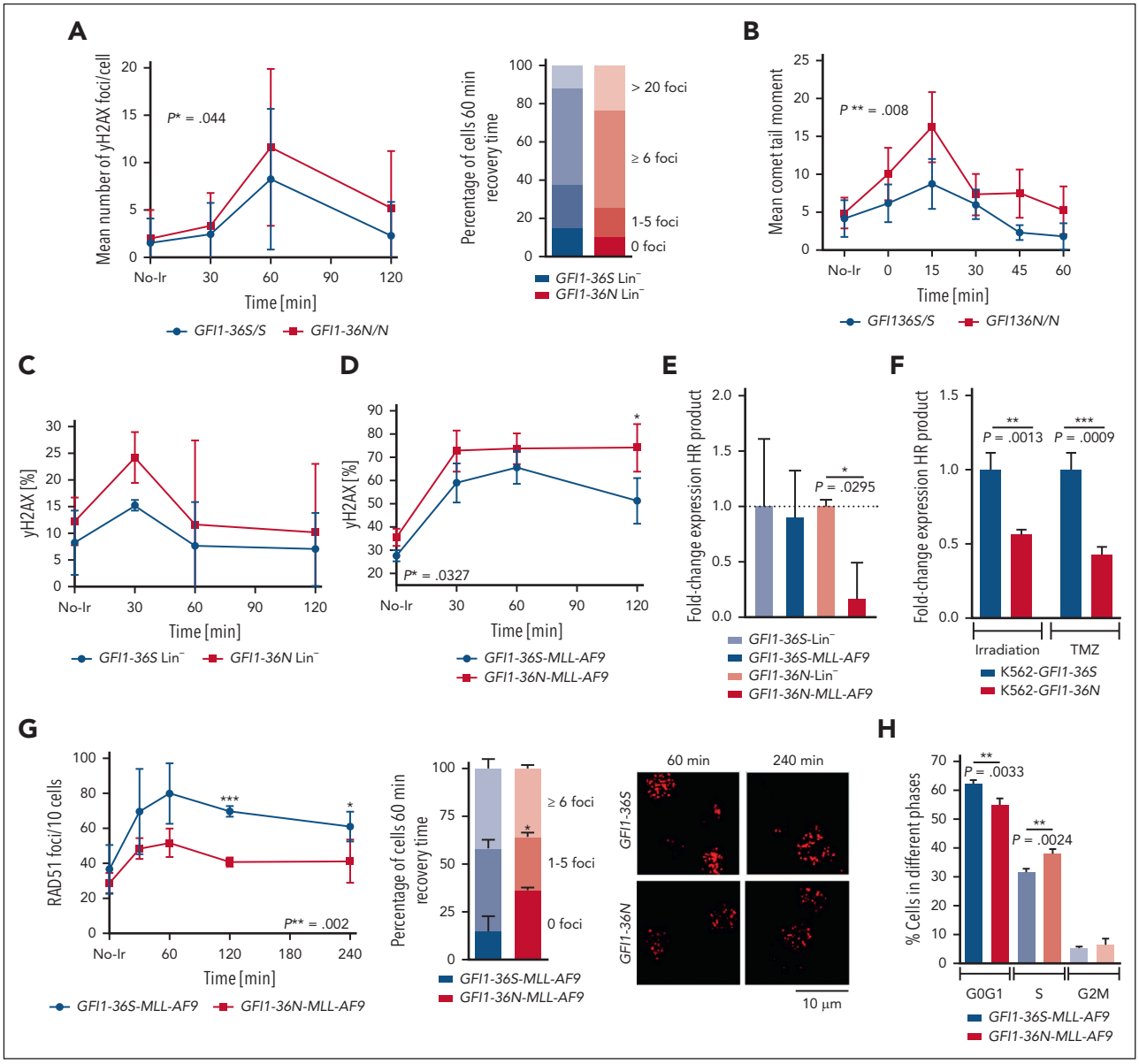

Figure 3. Higher DNA damage in *GFI1-36N* cells and lower DNA repair in *GFI1-36N* leukemic cells. (A) γH2AX-assay results of *GFI1-36S* and *GFI1-36N* thymocytes. γH2AX foci were stained with an antibody against γH2AX (immunofluorescence staining) and counted at different time points after 2 Gy irradiation. The images were analyzed with Imaris. Approximately 50-176 cells per sample; mean ± standard deviation (SD). *P* value was calculated over time. (B) Alkaline comet assay results of *GFI1-36S* and *GFI1-36N* thymocytes at different time points after irradiation with 5 Gy. Tail moment was analyzed from 34-65 cells per sample with the Comet-Assay Software from CaspLab. Mean ± SD. *P* value was calculated over time. (C) Murine nonleukemic progenitor cells (Lin⁻ cells) or (D) leukemic (*MLL-AF9*) BM cells from mice that received transplantation were irradiated with 3 Gy and were analyzed by flow cytometry at different time points after irradiation γH2AX level. n = 3; mean ± SD. (E) HR assay results from murine *GFI1-36S*- (n = 2) and *GFI1-36N*- (n = 2) Lin⁻ cells and murine GFI1-36S- (n = 2) and GFI1-36N- (n = 2) *MLL-AF9* BM cells. The HR rate was measured with RT-PCR after the cells were transfected with 2 plasmids of the plasmid-based homologous recombination assay from Norgen Biotek Corp; mean ± SD (F) K562 cell lines expressing *GFI1-36S* or *GFI1-36N* were generated by CRISPR/Cas. The HR rate was measured as described in (E) 2 hours after irradiation with 3 Gy or 24 hours after treatment with 100 µg/mL temozolomide (TMZ). N = 3, mean ± SD (G) RAD51 foci formation in murine *GFI1-36S* and *GFI1-36N* leukemic (*MLL-AF9*) BM cells was analyzed at different time points after irradiation with 5 Gy. n = 3 (31-73 cells per sample), mean ± SD. **P* > .05; ***P* < .01; ****P* < .001. (H) Cell-cycle analysis of *GFI1-36S* and *GFI1-36N MLL-AF9* cells. *GFI1-36S*: n = 3 and *GFI1-36N*: n = 4; mean ± SD. ***P* < .01. No-Ir: no irradiation (0 Gy).

human AML cells were plated in 1 mL MethoCult media (H4434, Stemcell) in 6-well plates, and the colonies were counted after 10 days of incubation. To measure the cell viability, metabolic activity was assessed using the 3-(4,5-dimethylthiazol-2-yl)-2,5-diphenyltetrazolium bromide (MTT) assay (Abcam), which was performed according to the manufacturer's protocol. For the MTT assay, cells were plated at a density of 3×10^5 cells per mL, and temozolomide was added in a range between 5 µg/mL and 400 µg/mL and incubated at 37°C and 5% CO_2 for 48 hours. After the drug treatment, the media was replaced with MTT reagent and incubated for 3 hours, followed by MTT solvent for 15 minutes. The absorption was measured at 590 nm using a Victor X3 Multimode Plate Reader (Perkin Elmer). For in vivo drug treatments, working solutions of 10 mg/mL temozolomide and 20 mg/mL olaparib were prepared freshly on the day of treatment with PBS. Mice were treated intraperitoneally according to their weight

Downloaded from http://ashpublications.net/blood/article-pdf/142/25/2175/2177539/blood_bld-2022-015752-main.pdf by guest on 03 May 2024

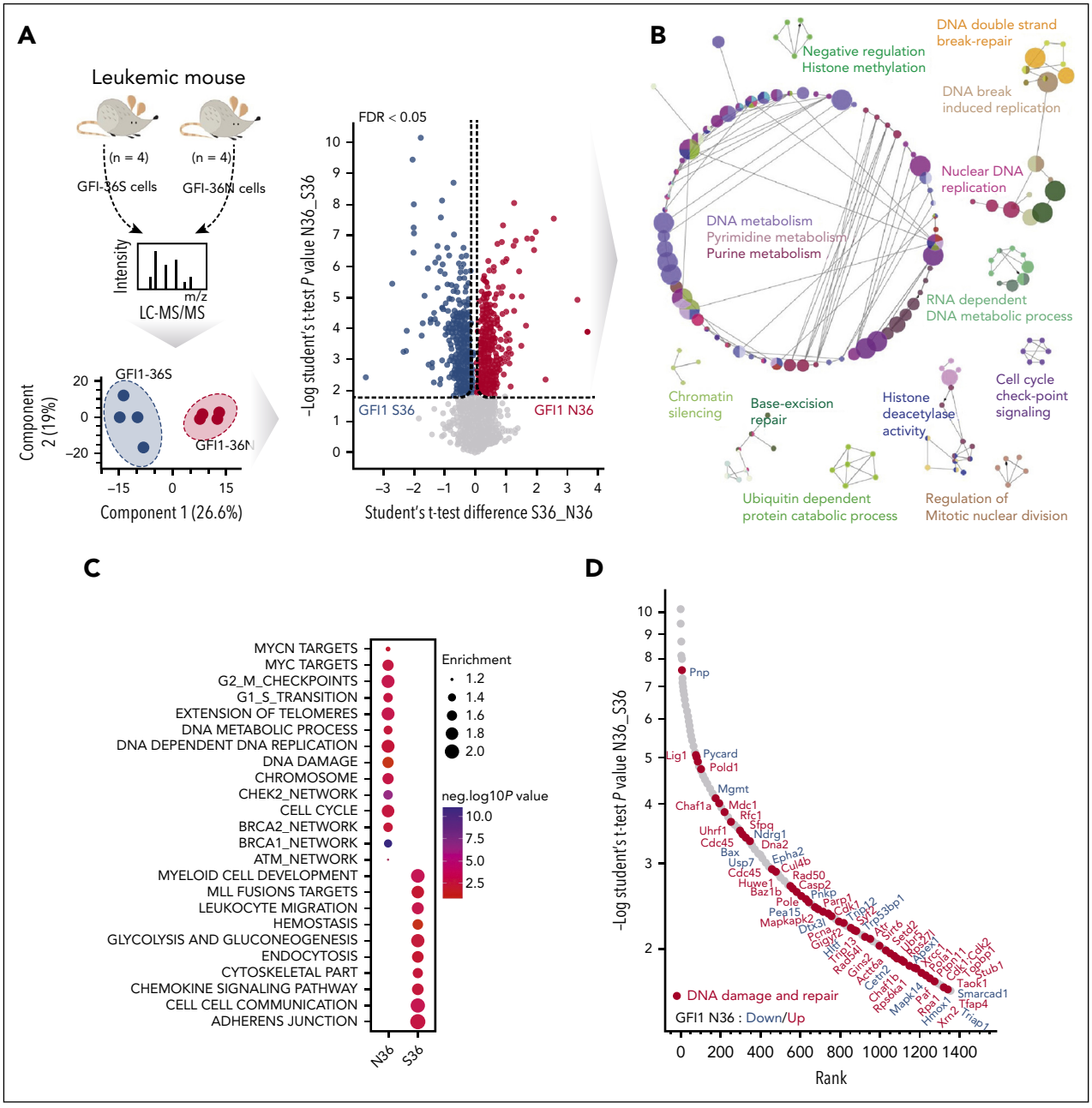

Figure 4. Proteome discovers *GFI1-36N* leukemic cells deregulate DNA repair protein MGMT. Proteomic analysis of primary murine and human *GFI1-36S* and *GFI1-36N* leukemic cells (A) Schematic representation of the experimental setup of murine *GFI1-36S* (n = 4) vs *GFI1-36N* (n = 4) leukemic BM cells proteome experiment, principle component analysis of measured samples, and evaluation of the results (left). Volcano plot displays significantly regulated proteins (permutation-based FDR < 0.05) is shown (right). (B) Network analysis of significantly regulated proteins between the 2 genotypes using Cytoscape. The network displays enriched Gene Ontology Biological Processes terms ($P < .01$). (C) Dot plot showing the significantly enriched GFI1-36N and GFI1-36S specific gene set enrichment terms based on proteomic analysis (D) Rank plot displaying the total number of DNA damage and repair proteins (highlighted with red dots) of all significantly regulated proteins in the data set. (E) Significantly regulated DNA damage and repair proteins grouped according to their specific pathways (selected from panel D). Rank plot displaying all significantly regulated proteins in GFI1 36N and 36S leukemia cells. The protein that participates in DNA damage repair are highlighted in red dots. The GFI1 36N upregulated proteins are marked in red, and downregulated proteins are marked in blue. The x-axis denotes the protein rank and y-axis denotes the –log10 *P* value. (F) Venn diagram showing the unique and shared number of differentially expressed proteins in murine and human AML samples (also see supplemental Figure 4H). MGMT is 1 of the shared and significantly altered proteins in both mouse and human samples. (G) Violin plot showing the log2 intensity of MGMT protein level in primary *GFI1-36S* (n = 4) vs *GFI1-36N* (n = 4) murine leukemic BM cells. (H) Violin plot showing the log2 intensity of MGMT protein level in human *GFI1-36S* (n = 11) vs *GFI1-36N* (n = 9) cells from patients with AML patient.

with olaparib and with temozolomide (temozolomide 50 mg/kg [days 2-4] and olaparib 100 mg/kg [days 2-3]). The procedure was repeated if mice were deemed suitable according to their status and scoring.

Statistical analysis

GraphPad Prism 6 was used for the statistical analyses. Significance was calculated using paired or unpaired two-sided *t* tests.

Downloaded from http://ashpublications.net/blood/article-pdf/142/25/2175/2177539/blood_bld-2022-015752-main.pdf by guest on 03 May 2024

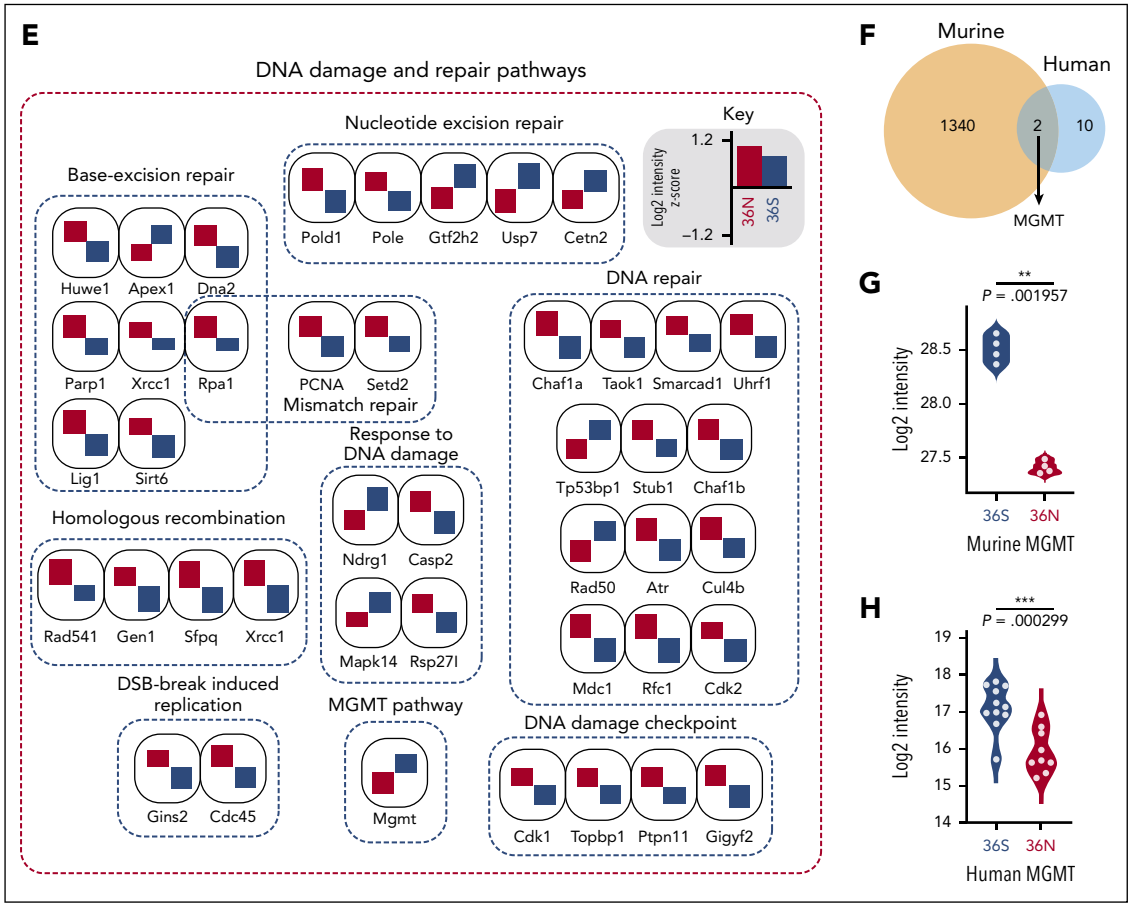

Figure 4 (continued)

Clinical trial NCT04207190

This phase 1/1b trial studies the safety profile and potential efficacy of talazoparib in combination with gemtuzumab ozogamicinin CD33-positive patients with AML who are relapsed or refractory. Patient samples were genotyped as previously described.[6]

Routine protocols and procedures are described in detail in supplemental Methods.

Results

Presence of *GFI1-36N* is associated with increased DNA damage and compromised DNA repair

The presence of a *GFI1-36N* allele was associated with an increased frequency of chromosomal aberrations in 3 cohorts of patients with AML (Essen, Dresden, and Hannover) independent of age, sex, and French American British (FAB) classification (Figure 1A-B; supplemental Tables 1 and 2). The allele did not correlate with a particular molecular alteration, confirming our previous observations for patients with MDS.[7] The demographic details, FAB type, blood analysis, and mutational status of the Hannover patient cohort are shown in supplemental Tables 3 to 8. To gain further molecular insight, we used *GFI1-36S* and *GFI1-36N* knockin mice.[9,17] We generated *GFI1-36S* or *GFI1-36N* myeloid leukemia cells expressing the MLL-AF9 oncofusion protein[25] and performed 4 rounds of serial transplantation to allow sufficient time for the effects of reduced DNA repair capacity to become detectable (Figure 1C). The frequency of deletions, insertions, and mutations was significantly higher in *GFI1-36N* than those in *GFI1-36S* leukemic cells (Figure 1D). Furthermore, *GFI1-36N* leukemic cells showed more missense mutations than *GFI1-36S* leukemic cells (Figure 1E), but the frequency of large-scale chromosomal aberrations remained the same in both types of leukemic cells (supplemental Figure 1A). However, microdeletions (detected by array–comparative genomic hybridization) were observed more frequently in *GFI1-36N* leukemic cells, with 3.33 ± 0.33 more microdeletions than *GFI1-36S*–expressing leukemic cells (supplemental Figure 1B) but did not reach significance, likely because of the small sample size. To confirm our results, we used an additional murine AML model that causes insertional mutagenesis specifically in hematopoietic cells by means of a transposon-transposase system (Figure 1F),[23] allowing for the targeted sequencing of the genomic areas to which the transposon has been relocated. The presence of *GFI1-36N* was associated with a significantly increased number of common insertion sites of the transposon compared to *GFI1-36S*–expressing cells (Figure 1G). *GFI1-36N*–associated insertion sites were frequently found proximal to genes involved in DNA repair such as *TRIM44*, *MECOM*, and *ZEB2* (supplemental Figure 2A). The presence of *GFI1-36N* correlated with clonal aberrant karyotypes, yet the overall sample number was too low to gain statistical significance (supplemental Figure 2B).

Downloaded from http://ashpublications.net/blood/article-pdf/142/25/2175/2177539/blood_bld-2022-015752-main.pdf by guest on 03 May 2024

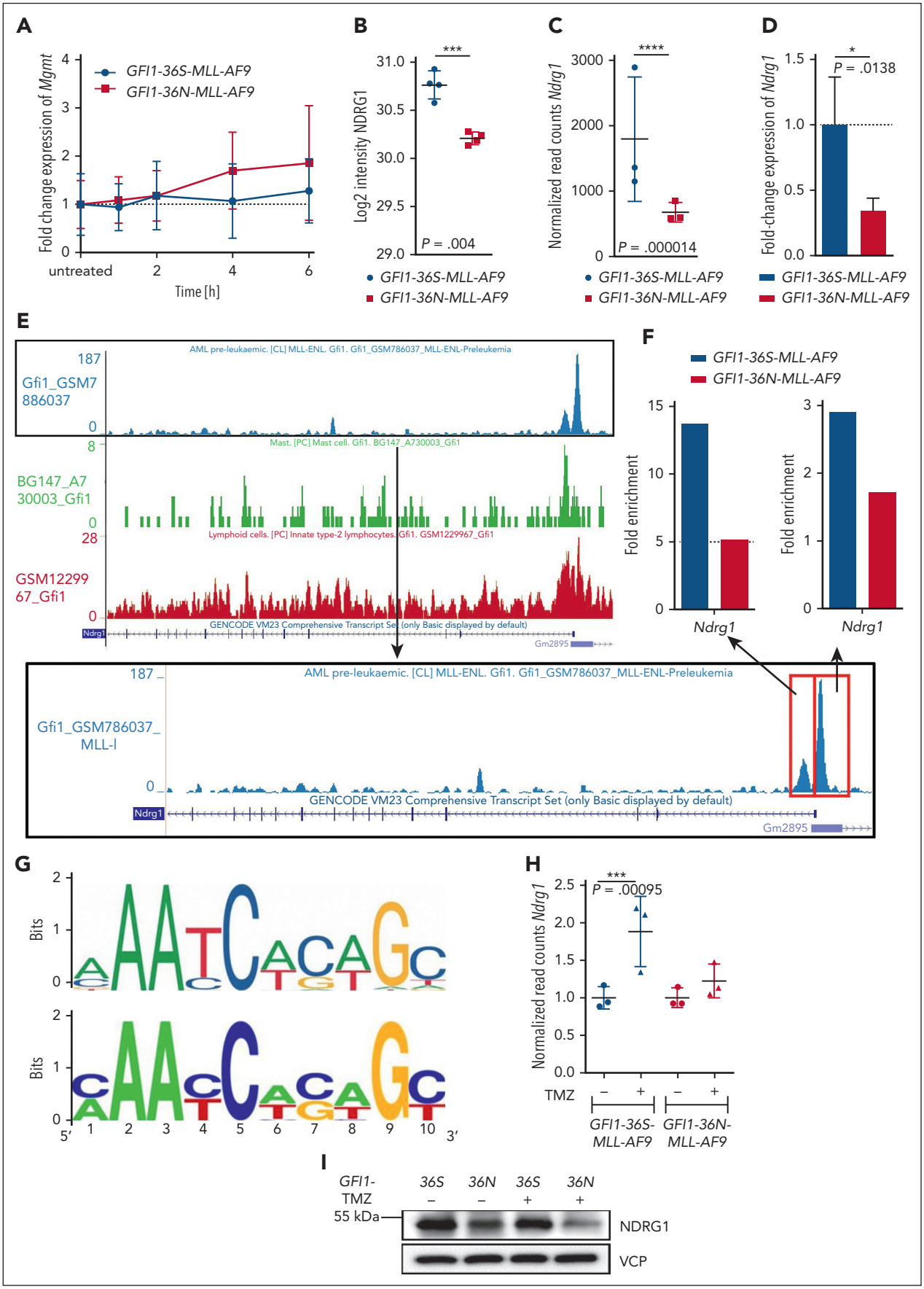

Figure 5.

Downloaded from http://ashpublications.net/blood/article-pdf/142/25/2175/2177539/blood_bld-2022-015752-main.pdf by guest on 03 May 2024

We determined the mutational signature of murine *GFI1-36S* and *GFI1-36N* leukemic cells from our MLL-AF9 model, performing analyses on synonymous and nonsynonymous variants and identifying 2 different clusters (k = 2; Figure 2A). Matching the corresponding signatures to Catalogue of Somatic Mutations in Cancer (COSMIC) signatures,[27] both signatures (Sig1 and Sig2) were similar to single-base substitution 5 (SBS5; similarity > 0.70), which is potentially associated with mutational processes related to aging and nucleotide excision repair. However, each mouse line (*GFI1-36N* and *-36S*) was matched to a different subtype of SBS5 (Figure 2C), mainly driven by different adjacent bases (5′ and 3′ of the mutation) of C>T and T>C mutations (Figure 2B).

To test whether these results can be recapitulated in humans, a cohort of 1530 patients diagnosed with AML or MDS with 182 carriers of the *GFI1-36N* variant was investigated. Using de novo mutational signature identification for these 182 patients, we identified 4 different signatures (Figure 2D; supplemental Figure 3A-B). Sign.01 likely has a technical origin, because we see it consistently in other cohorts as well. However, Sign.02, Sign.03, and Sign.04 showed similarity to COSMIC reference signatures SBS6, SBS5, SBS1, and SBS87 (Figure 2E) and were similar to Sig1 and Sig2 observed in murine samples (Figure 2B). A comparison of the murine and human results indicated that there are signatures in both data sets that are based on C>T mutations and, to a lesser extent, on T>C (Figure 2B,D).

To further investigate global DNA damage response and repair, we first used murine thymocytes, an immune cell type expressing higher levels of GFI1 than BM cells, and tested their response to DNA damage with comet assays and by measuring γH2AX foci after exposure to irradiation. An 80% increased tail moment and a 40% higher number of γH2AX foci (both $P \leq .05$) were observed in *GFI1-36N* thymocytes than in *GFI1-36S* cells (Figure 3A-B). However, the slope of the decreasing number of foci and tail moment during the repair phase was similar between *GFI1-36N* and *GFI1-36S*–expressing cells. In addition, *GFI1-36N* Lin$^-$ cells from the mouse BM showed a higher number of γH2AX foci than *GFI1-36S* control cells, but both cell types had a similar rate of DNA repair slope (Figure 3C). Although leukemic *GFI1-36N* cells also demonstrated higher DNA damage upon exposure to the same dose of irradiation compared with leukemic *GFI1-36S* control cells, they showed a reduced DNA repair capacity compared with *GFI1-36S* leukemic cells (Figure 3D).

We first performed an assay to follow homologous recombination (HR) with a polymerase chain reaction (PCR) approach.[28] Murine *GFI1-36N* leukemic cells had a 75% diminished capacity for HR compared with *GFI1-36N* nonleukemic Lin$^-$ progenitor cells, *GFI1-36S MLL-AF9* leukemic cells, or *GFI1-36S* nonleukemic Lin$^-$ progenitor cells (Figure 3E). To confirm this observation in an independent human leukemia model, K562 cell lines with 1 *GFI1-36N* allele were generated using CRISPR/Cas. Upon irradiation or treatment with the alkylans temozolomide, K562 cells with a *GFI1-36N* allele showed reduced HR repair capacity compared with cells carrying both *GFI1-36S* alleles (Figure 3F). This diminished rate of HR in the murine or human models was not due to reduced expression of RAD51 (a key HR facilitator)[29-31] at steady state (supplemental Figure 3C). To check whether a potentially different binding between GFI1-36S and GFI1-36N with RAD51 could explain the detected impeded HR and the different RAD51 foci formation in GFI1-36N leukemic cells, we performed immunofluorescence experiments, and we did not observe a different colocalization of GFI1-36S or GFI1-36N with RAD51 (supplemental Figure 3D). However, the number of RAD51 foci appearing after 5 Gy irradiation was significantly reduced in *GFI1-36N* leukemic cells compared with that in *GFI1-36S* leukemic cells, confirming the results obtained with the plasmid-based HR assay (Figure 3G).

53BP1 regulates the double-stranded break repair pathway choice between HR and nonhomologous end joining (NHEJ) by promoting the NHEJ S phase.[31] We probed the formation of 53BP1 foci but did not find significant differences between *GFI1-36S* and *GFI1-36N* leukemic cells (supplemental Figure 3E) nor a colocalization between GFI1 and 53BP1 (supplemental Figure 3F), indicating that the capacity for NHEJ remained unchanged in the presence of the variant *GFI1* allele. Coordinated DNA repair depends on proper control of cell-cycle status, and HR-directed DNA repair occurs mostly in G2 or S phases. The observed reduction of HR-directed DNA repair in the presence of a *GFI1-36N* allele was not due to a reduction of cells in the S or G2/M phases. On the contrary, a higher proportion of *GFI1-36N* leukemic cells was in S phase compared with *GFI1-36S* leukemic cells (Figure 3H), suggesting a direct involvement of the GFI1 variant of the DNA repair machinery.

Presence of *GFI1-36N* deregulates MGMT levels

Using in-depth quantitative proteome analysis of murine *GFI1-36S* and *GFI1-36N* leukemic cells (n = 4, biological replicates. Figure 4A), we quantified nearly 7000 proteins at a peptide and protein false discovery rate of 1%, of which we found 1353 proteins to be differentially regulated (permutation-based false discovery rate [FDR] < 0.05; Figure 4A; supplemental Data 1) between the genotypes. We then performed biological process and pathway enrichment analysis using Cytoscape. DNA metabolism, DNA double-strand break and repair, DNA damage and repair pathway, base excision repair pathway, chromatin

Figure 5. MGMT downregulation in *GFI1-36N* cells due to low levels of NDRG1. (A) Fold change expression of *Mgmt* in murine *GFI1-36S*- and *GFI1-36N-MLL-AF9* leukemic BM cells at different time points after actinomycin D (10 μg/mL) treatment. *Mgmt* level was normalized to *Hprt* and to the untreated controls. n = 3; mean ± SD. (B) NDRG1 protein level in *GFI1-36S*- and *GFI1-36N-MLL-AF9* leukemic BM cells (proteomic). n = 4; mean ± SD. (C) *Ndrg1* expression (normalized read counts; RNA-seq) of murine leukemic *GFI1-36S*- and *GFI1-36N-MLL-AF9* BM cells. n = 3; mean ± SD. (D) *Ndrg1* gene expression measured in *GFI1-36S*- and *GFI1-36N-MLL-AF9* BM cells by RT-PCR. *GFI1-36S*: n = 3 and *GFI1-36N*: n = 3; mean ± SD. (E) Published GFI1-ChIP-seq data sets showing the *Ndrg1* gene and its regulatory elements with the possible binding sides of GFI1 (red square) at regulatory elements of *Ndrg1*. (F) GFI1-ChIP-quantitative PCR of the *Ndrg1* upper regulatory elements of murine *GFI1-36S* and *GFI1-36N* leukemic BM cells. *Gapdh* and *Runx1* were used as a control (right). (G) Comparison between the GFI1 binding motif from the Jasper database (top) and the consensus motif found using find individual motif occurrence (FIMO) at sites occupied by GFI1 in 21 genes differentially expressed in granulocyte/monocyte progenitors s from *GFI1-36N* or *-36S* animals. (H) *Ndrg1* expression (RNA-seq) in murine leukemic *GFI1-36S*- and *GFI1-36N-MLL-AF9* cells after treatment with 50 μg/mL TMZ for 20 hours and without. Normalized read counts of treated samples were normalized to the untreated samples. n = 3; mean ± SD. (I) NDRG1 protein level was analyzed by immunoblotting in BM cells from *GFI1-36S* and *GFI1-36N* leukemic mice without and with TMZ (50 μg/mL) treatment for 24 hours. *$P < .05$; ***$P < .001$; ****$P < .0001$.

Downloaded from http://ashpublications.net/blood/article-pdf/142/25/2175/2177539/blood_bld-2022-015752-main.pdf by guest on 03 May 2024

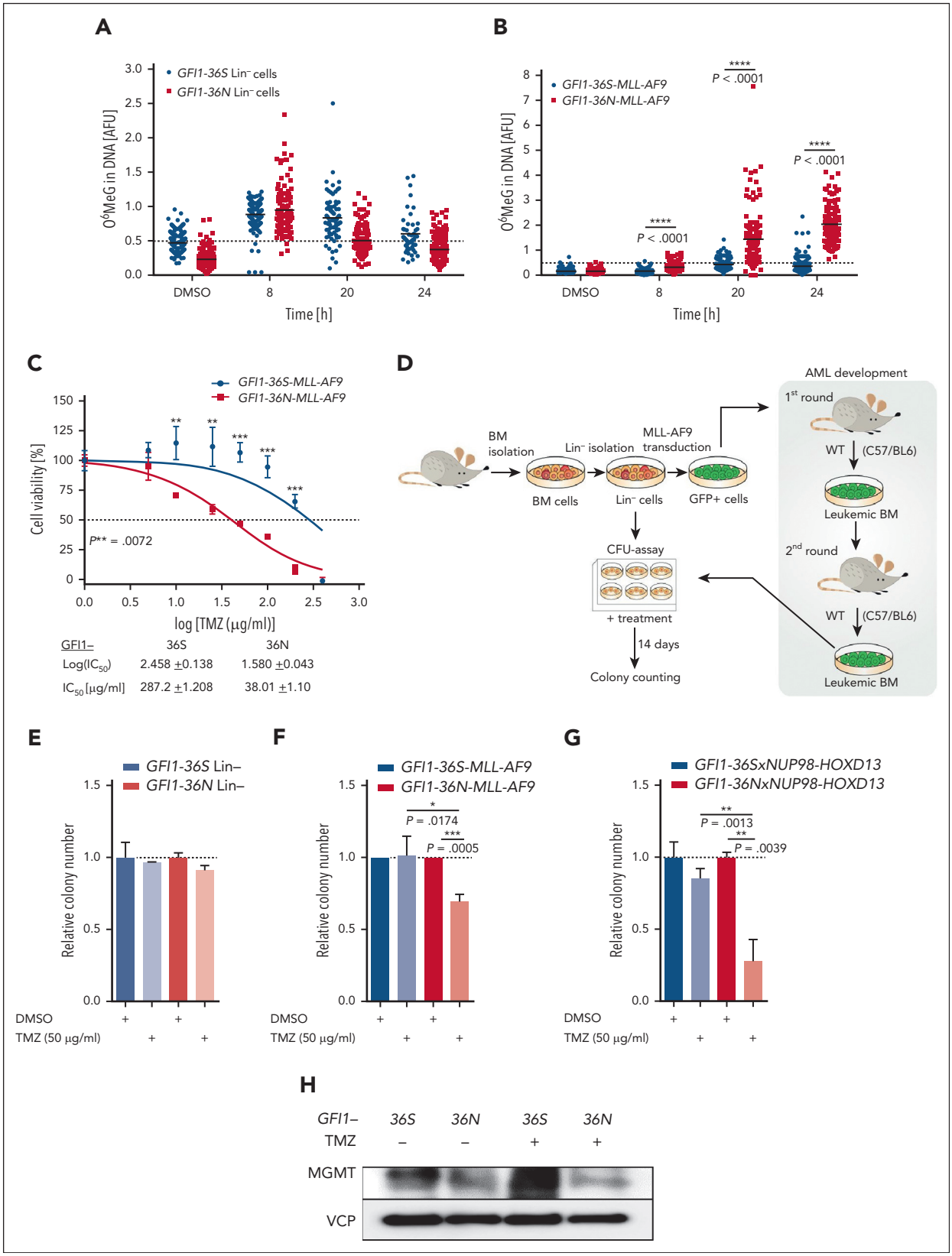

Figure 6. GFI1-36N leukemic cells are highly susceptible to TMZ treatment. (A) Functional Mgmt assays from murine *GFI1-36S* and *GFI1-36N* Lin⁻ cells (45-206 cells per sample) and (B) *GFI1-36S* and *GFI1-36N MLL-AF9* BM cells from mice that received transplantation (115-223 cells per sample). Cells were treated with 100 µg/mL TMZ and at different time points after treatment O^6MeG level was analyzed with immunofluorescence. The ACAS program was used for the evaluation. (C) Cell viability of murine *GFI1-36S* and *GFI1-36N MLL-AF9* BM cells measured by MTT assay after treatment with different TMZ concentrations for 48 hours, and IC_{50} values were calculated; mean ± SD. (D) Schematic experimental setup of the colony-forming unit (CFU) assays. (E) Murine *GFI1-36S* and *GFI1-36N* Lin⁻ cells and (F) *MLL-AF9* BM cells from mice were plated for 14 days in methylcellulose medium with the addition of 50 µg/mL TMZ or as a control dimethyl sulfoxide (DMSO). The colony number of the treated samples was calculated

Downloaded from http://ashpublications.net/blood/article-pdf/142/25/2175/2177539/blood_bld-2022-015752-main.pdf by guest on 03 May 2024

silencing, and cell-cycle checkpoint signaling (Figure 4B) were among these pathways, and this was in congruence with the functional data presented in Figure 3 regarding these processes. We found DNA damage, cell-cycle, cellular Myc (c-Myc) targets, CHEK2 network, ataxia-telangiectasia mutated (ATM) network, BRCA1 and -2 network specifically enriched in a GFI1-36N–dependent fashion (Figure 4C), suggesting that *GFI1-36N* cells undergo extensive DNA damage and repair. We focused then on DNA damage and repair pathways and could identify 66 proteins that were either upregulated or downregulated depending on the presence of *GFI1-36N* (Figure 4D, permutation-based FDR < 0.05). Most of the DNA damage-sensor proteins were upregulated in *GFI1-36N* leukemic cells (Figure 4E), supporting the notion that these cells experience more DNA damage than *GFI1-36S* leukemic cells.

To explore whether these changes might be explained by altered gene expression, we first performed RT2 profiler PCR arrays for DNA repair genes and observed that 40 out of 84 genes were differentially expressed (supplemental Table 9). We further confirmed this by bulk transcriptome analysis on BM cells from leukemic *GFI1-36S* and *GFI1-36N* mice (MLL-AF9 model). A gene set enrichment analysis revealed differentially expressed genes belonging to the DNA repair and p53 pathways and genes such as *Gen1*, *Cul4b*, and *Dna* (supplemental Figure 4A-C), although not all genes deregulated in the RT2 approach were deregulated in the RNA sequencing (RNA-seq) approach and vice versa.

The enzyme O^6-methylguanine-DNA-methyltransferase (MGMT) catalyzes the transfer of methyl groups from O(6)-alkylguanine in the DNA to itself, thereby repairing these lesions.[32] MGMT was among the most downregulated protein and transcript levels in GFI1-36N leukemic cells compared with that in GFI1-36S leukemic cells (Figure 4D-E; supplemental Figure 4D-F). The *Mgmt* RNA and protein expression remained unchanged in nonleukemic progenitor cells expressing *GFI1-36S* or *-36N* (supplemental Figure 4G-H), suggesting that the leukemic condition contributed to the reduced expression of *Mgmt* and Mgmt. To further explore this, we performed a deep proteome analysis of samples of patients with AML (genotypes *GFI1-36S* [n = 11] and *GFI1-36N* [n = 9]). The details of the patient samples used for proteomics analysis are listed in supplemental Tables 10 and 11). We profiled 165 patients with AML to identify 9 samples as *GFI1-36N* heterozygous carriers. The samples were selected evenly across disease stages and cytogenetic groups to counteract a potential subtype-specific bias. From a total of 8027 proteins identified, 6058 proteins were quantified in 70% of at least 1 genotype; significant analysis found 12 proteins were differentially regulated (permutation-based FDR < 0.05; details in supplemental Methods) between the 2 genotypes (supplemental Figure 4I; supplemental Data 2), and these include poly-ADP ribose polymerase (PARP) 14, KIN, HAUS5, and RAD18, involved in DNA damage, genome stability, and the DNA-binding protein PAPD5. Of these, 2 proteins were shared between murine and human samples (Figure 4F). Both murine and human AML samples showed downregulated Mgmt/MGMT levels in leukemic *GFI1-36N* cells compared with *GFI-36S* cells (Figure 4G-H). This strongly suggests that the expression of MGMT is reduced in AML cells expressing *GFI1-36N*, both at the RNA and protein levels. We further confirmed our findings in a published AML proteome data set of 177 samples.[33] The *GFI1-36N* were identified by single nucleotide variant calling using the RNA-seq data (supplemental Figure 4J) and compared those for all *GFI1-36S* samples or the top 10 most *GFI1*-36S–expressing samples for equal variance comparison (supplemental Figure 4K-L).

Of note, we assessed the 66 DNA damage repair proteins and their transcript regulation systematically by correlation analysis. In general, the overall and genotype-specific sample transcriptome-to-proteome correlation was Pearson R = 0.46 to 0.48 (supplemental Figure 5A-C; supplemental Data 3), similar to that of our previous work.[34] We performed comparative analysis to find shared and unique genes between the data sets (supplemental Figure 5D). The gene ontology enrichment analysis identified genes changing in both RNA proteins that are enriched for protein binding, translation, ribosomal RNA processing, ribosome subunits, DNA break and repair pathway, and caspase complex (supplemental Figure 5E). In the transcript only, upregulated genes enrich for terms such as protein binding, ribonucleo protein complex, noncoding RNA processing, messenger RNA processing, and splicing (supplemental Figure 5F). Genes upregulated at the protein but not at the transcript level were enriched for response to stress, translation, DNA replication, DNA repair proteins, the MCM complex, histone modifications, and catalytic activity (supplemental Figure 5G). This analysis points out that the DNA break and repair pathways are subjected to changes, as reflected in both RNA-protein levels in our data set. A direct transcriptome-proteome correlation suggests MGMT might not be regulated by posttranscriptional regulation (supplemental Figure 5H). However, when looking at the 66 selected DNA damage repair proteins in both the overall and genotype-specific transcriptome-to-proteome correlation, the data suggest some of these genes might undergo posttranscriptional regulation (supplemental Figure 5I-K; supplemental Data 3) because their transcript abundance correlates inversely to protein.

NDRG1 regulates MGMT levels in *GFI1-36N* AML cells

We next investigated why the presence of GFI1-36N in leukemic cells leads to lower levels of Mgmt/ MGMT. An altered methylation status of the *MGMT* promoter was not the reason (supplemental Figure 6A-C),[35,36] nor does GFI1 bind to regulatory elements of the MGMT locus, based on published chromatin immunoprecipitation (ChIP)-seq data sets from CODEX (GSE31657, GSE69101, GSE50806, and GSE42518).[17,33,37,38] The presence of *GFI1-36N* also had no effect on the RNA stability of *Mgmt* of murine *GFI1-36S* and *-36N* leukemic cells (Figure 5A). The GFI1 interactome (using mass spectrometry [AP-MS]) revealed known interactors, such as Histon deacetylase and protein-arginine methyltransferase 1 but did not reveal a direct interaction of GFI1 with MGMT (supplemental Figure 6D-F).

Figure 6 (continued) relative to the control. n = 3; mean ± SD. (G) CFU assay was performed with malignant BM cells from transgenic *GFI1-36S*x and *GFI1-36NxNUP98-HOXD13* mice. Cells were treated with 50 µg/mL TMZ and as a control with DMSO. The colony number after 14 days in culture of the treated samples was calculated relative to the control. n = 2, each triplicate, mean ± SD. (H) MGMT protein level was measured by immunoblotting in BM of *GFI1-36S* and *GFI1-36N* leukemic mice without and with TMZ (50 µg/mL) treatment for 24 hours. *P < .05; **P < .01; ***P < .001; ****P < .0001. AFU, arbitrary fluorescence units (O^6MeG/4′,6-diamidino-2-phenylindole); IC_{50}, 50% inhibitory concentration.

Downloaded from http://ashpublications.net/blood/article-pdf/142/25/2175/2177539/blood_bld-2022-015752-main.pdf by guest on 03 May 2024

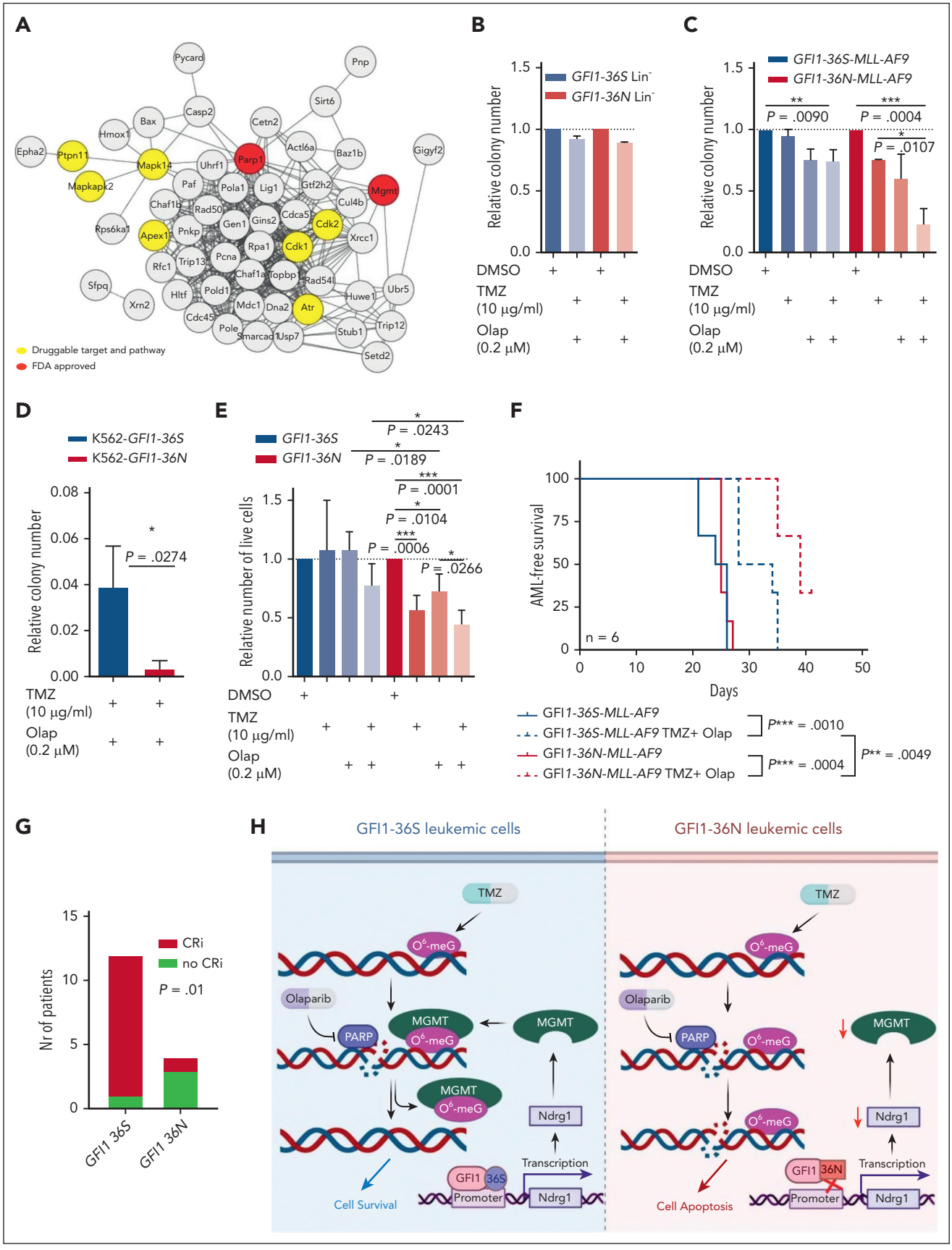

Figure 7. The combination of TMZ and olaparib shows synergistic effect on *GFI1-36N* leukemic cells in vitro and in vivo. (A) Analysis of possible drug targets of the differently expressed DNA repair–related proteins (results from the proteomic analysis of *GFI1-36S* and *GFI1-36N* leukemic BM cells). (B) CFU assay results of murine Lin⁻ cells

Downloaded from http://ashpublications.net/blood/article-pdf/142/25/2175/2177539/blood_bld-2022-015752-main.pdf by guest on 03 May 2024

NDRG1 (stress-responsive protein involved in DNA damage response) positively regulates and stabilizes MGMT in human glioblastoma cells by direct protein-protein binding.[39,40] NDRG1 protein levels were reduced in GFI1-36N leukemic cells (Figure 5B). Additionally, using our RNA-seq data sets from murine leukemic cells, the expression of Ndrg1 was also significantly lower in GFI1-36N leukemic cells than in GFI1-36S leukemic cells (Figure 5C). We validated these results using reverse transcription PCR (Figure 5D). Reanalysis of published GFI1 ChIP-seq data from CODEX (GSE31657, GSE69101, GSE50806, and GSE42518)[17,33,37,38] revealed 2 potential GFI1 binding sites at the upper regulatory regions of Ndrg1 in 3 out of 4 data sets (Figure 5E). Although GFI1 has been described as a transcriptional repressor, it can also act as an activator, as demonstrated in the case of medulloblastoma[41] or in T-cell leukemia for Ikaros.[42,43] Using ChIP–quantitative PCR with a GFI1 targeting antibody, we found that GFI1-36S bound to a higher degree to both upper regulatory elements of Ndrg1 than GFI1-36N in murine leukemic cells (Figure 5E-F). Repeated attempts to examine the binding of GFI1-36S and GFI1-36N on a genome-wide level did not yield sufficient reads; hence, this must be done in future studies. In line with this, PNKP and APEX1, 2 additional proteins bound and stabilized by NDRG1,[39] were downregulated at both RNA and protein levels in GFI1-36N compared with in GFI1-36S leukemic cells (supplemental Figure 6G-H). To assess whether decreased binding of GFI1-36N to its target genes was due to a different binding sequence, we analyzed genes differentially expressed between granulocyte/monocyte progenitors from animals carrying either GFI1 variant. The consensus binding sequence of GFI1-36S and GFI1-36N was not different based on selected 21 genes with a GFI1 peak using the program FIMO (Figure 5G)[44] and almost identical to the published GFI1-binding consensus motif.[45]

Next, we treated *GFI1-36S* and *GFI1-36N* leukemic cells with temozolomide, leading to the upregulation of *Ndrg1* expression in *GFI1-36S* but not in *GFI1-36N* leukemic cells (Figure 5H), and this was confirmed at protein levels 24 hours after temozolomide treatment (Figure 5I). These data suggest that GFI1-36S more efficiently binds to regulatory elements in the *Ndrg1* locus than GFI1-36N and suggest that GFI1-36S occupation leads to increased *Ndrg1* expression. However, more future work is required to fully understand this.

Combination of temozolomide and olaparib is selectively cytotoxic to *GFI1-36N* leukemic cells in vitro and in vivo

The alkylating agent temozolomide methylates guanine residues at O-6 positions (O^6MeG). In a subset of patients with glioblastoma, DNA methylation of the *MGMT* locus promoter sequences leads to a downregulation of the MGMT protein level, which sensitizes the tumor cells to treatment with temozolomide.[32,35,36] A reduced level of MGMT could open the possibility of targeting *GFI1-36N*–expressing leukemic cells. To probe for this, we explored MGMT-mediated clearance of O^6MeG adducts induced by temozolomide but found no difference in nonleukemic Lin^- cells of *Gfi1-36S* and *-36N* knockin mice (Figure 6A). However, *GFI1-36N* leukemic cells showed significantly lower efficiency to repair O^6MeG than *GFI1-36S* leukemic cells (Figure 6B). The 50% inhibitory concentration value of temozolomide was eightfold lower in leukemic *GFI1-36N* cells than in leukemic *GFI1-36S* cells (Figure 6C). At low concentrations, temozolomide did not affect the expansion of nonleukemic hematopoietic cells (Figure 6D-E; supplemental Figure 7A), but at these same concentrations, temozolomide significantly inhibited the growth of leukemic *GFI1-36N* cells and caused extensive apoptosis (Figure 6F; supplemental Figure 7B-D). RNA-seq data showed that *GFI1-36N* leukemic cells were enriched for gene set enrichment analysis terms related to p53 pathway activation and apoptosis after 20 hours of treatment with temozolomide compared with *GFI1-36S* leukemic cells (supplemental Figure 8). We validated these findings in another murine AML model in which *GFI1-36N* or *GFI1-36S* cells were generated that coexpressed the AML oncofusion protein NUP98-HOXD13. Similar to the previously generated *MLL-AF9*–expressing cells, these *NUP98-HOXD13* leukemic cells were more sensitive toward temozolomide when the *GFI1-36N* allele was present compared with the *GFI1-36S* allele (Figure 6G; supplemental Figure 9A). Further on, *GFI1-36S* leukemic cells upregulated MGMT levels after temozolomide treatment, which was not the case for *GFI1-36N* leukemic cells (Figure 6H).

We performed a network analysis of deregulated DNA repair proteins and queried for drugs targeting either the proteins or repair pathways. In this analysis, we found that the use of temozolomide to target MGMT repair pathways or olaparib to target PARP1 would be a possible approach (see details in supplemental Methods for data analysis and bioinformatics; Figure 7A). Olaparib can target cells with HR defects and potentiate the effect of temozolomide.[46-49] We observed that a combination of temozolomide and olaparib caused increased apoptosis in *GFI1-36S* leukemic cells in our system and significantly inhibited the growth of *GFI1-36N* leukemic cells compared with *GFI1-36S* leukemic cells without affecting nonleukemic cells in colony assays in vitro (Figure 7B,C; supplemental Figure 9B-E). We also confirmed this effect using K562 cells with a *GFI1-36N* allele or primary human AML cells from *GFI1-36N* carriers treated with TMZ and olaparib

Figure 7 (continued) after treatment with either the combination of 10 μg/mL TMZ and 0.2 μM olaparib (Olap) or DMSO as a control. n = 3, mean ± SD (C) CFU assay results from *MLL-AF9* BM cells from mice that received transplantation after treatment with either 10 μg/mL TMZ (n = 2), 0.2 μM Olap (n = 2), or the combination of both (n = 3, triplicate) and as a control DMSO (n = 3). Colony number was determined, and treated samples were calculated relative to the control. mean ± SD (D) CFU assay results from K562 cells expressing GFI1-36S and GFI1-36N, treated with 10 μg/mL TMZ and 0.2 μM Olap. Relative colony numbers were calculated with respect to DMSO control (n = 3, triplicate). (E) Primary human *GFI1-36S* (*GFI1-36S/S*: 2 × BM and 2 × peripheral blood) and *GFI1-36N* (*GFI1-36S/N*: 1 × BM and 1 × SPL and *GFI1-36N/N*: 2 × peripheral blood) cells from patients with AML were plated 14 days in methylcellulose media and treated as described in (B). Number of live cells was determined, and treated samples were calculated relative to the control. n = 4; mean ± SD. (F) AML-free survival of mice that received transplantatiob with TMZ and Olap treatment or without. *GFI1-36S* or *GFI1-36N MLL-AF9* BM cells were transplanted into sublethally irradiated WT mice and on day 3 after transplantation, the treatment with 100 mg/kg olaparib and 50 mg/kg TMZ was started. n = 6. (G) In an ongoing clinical trial (NCT04207190) of treating patients with AML with talazoparib along with gemtuzumab ozogamicin, 3 out of 4 GFI1-36N patients showed CRi, whereas 1 out of 12 GFI1-36S patients showed CRi. (H) Scheme elucidates GFI1-36N influence on DNA repair and genome stability in AML cells compared with GFI1-36S. *$P < .05$; **$P < .01$; ***$P < .001$. FDA, Food and Drug Administration; SPL, spleen. Scheme created with BioRender.com.

Downloaded from http://ashpublications.net/blood/article-pdf/142/25/2175/2177539/blood_bld-2022-015752-main.pdf by guest on 03 May 2024

(Figure 7D-E; supplemental Figure 9F). In both instances, *GFI1-36N* leukemic cells were highly sensitive to temozolomide, alone or in combination with olaparib. To characterize how the sensitivity to these compounds in *GFI1-36N* leukemic cells was mediated by downregulated MGMT levels, we assessed AML cell lines for MGMT expression. We performed lentiviral-mediated stable knockdown of *MGMT* in THP1 cells with the *GFI1-36S* genotype that showed abundant MGMT protein levels to mimic the phenotype (supplemental Figure 10A-C). Knockdown of *MGMT* in THP1 cells phenocopied the sensitivity to temozolomide or in combination with olaparib in cell growth and viability assays (supplemental Figure 10D). This is another indication that MGMT levels explain the sensitivity of *GFI1-36N* leukemic cells to DNA-damaging drugs. Additionally, we tested the sensitivity of GFI1-36N leukemic cells to standard chemotherapeutic agents. We treated another set of primary AML cells from the Dresden cohort (GFI1-36S, n = 15 and GFI1-36N, n = 11) with the drugs. We observed that GFI1-36N cells were more responsive to the drugs daunorubicin, gilteritinib, and venetoclax (supplemental Figure 11A-C), which might be related to the function of GFI1 regulating p53 and associated apoptosis signaling pathways.[50,51] However, there was no difference in the treatment response to the drugs cytarabine, azacytidine, sorafenib, and glasdegib (supplemental Figure 11D-G).

To recapitulate this in vivo, we transplanted *GFI1-36S-MLL-AF9* or *GFI1-36N-MLL-AF9* leukemic BM cells into sublethal irradiated wild-type mice and treated the mice with a combination of olaparib and temozolomide. The cohorts of treated mice with either genotype survived significantly longer than those that were untreated. However, the treated *GFI1-36N-MLL-AF9* mice survived significantly longer (mean, 7 days; $P = .0049$) than the *GFI1-36S-MLL-AF9*–treated mice (Figure 7F), again confirming the effect of *GFI1-36N* in sensitizing AML cells to combination treatment with olaparib and temozolomide. We also searched for clinical trials using temozolomide and/ or a PARP inhibitor. From 5 publicly recorded trials, 1 ongoing trial (NCT04207190) is examining talazoparib given together with gemtuzumab ozogamicin in patients with $CD33^+$ refractory or relapsed AML. In this cohort of patients, a statistically significant different response rate was observed, with only 1 of 12 patients with *GFI1-36S* homozygous showing complete remission with incomplete recovery (CRi) according to European Leukemia Network recommendation,[52] whereas 3 out of 4 patients with GFI1-36N heterozygous or homozygous achieved CRi during the course of treatment (Figure 7G).

Discussion

Alterations of DNA repair pathways contribute to the development of various solid cancer entities as well as hematologic malignancies.[53-56] GFI1 regulates DNA repair by coordinating the methylation of MRE11 and 53BP1. Consecutively, the loss of GFI1 affects HR but not NHEJ.[18] In line with this, *GFI1-36N* leukemic cells are compromised with regard to HR and MGMT but not for NHEJ-mediated repair. Molecularly, GFI1 transcriptionally regulates the activity of MGMT by activating the expression of NDRG1, a protein that stabilizes MGMT.[39] Although GFI1 has been originally described as a transcriptional repressor, it also associates with coactivators and other transcription factors, such as Ikaros, or with components of the nucleosome remodeling deacetylase complex to upregulate the expression of respective target genes.[42,43,57] GFI1-36N fails to bind to the same extent to regulatory elements of *Ndrg1* as GFI1-36S. This could explain the lower levels of MGMT in cells expressing the *GFI1-36N* variant and the failed upregulation of *Ndrg1* after treatment of *GFI1-36N*–expressing cells with temozolomide.

Both in human and murine cells, the presence of GFI1-36N is associated with a mutational signature because of an altered DNA-repair capacity. We also observed a higher susceptibility of *GFI1-36N* cells to DNA damage than of *GFI1-36S* cells. This might be partly due to more open chromatin as a result of increased H3K9 acetylation and H3K4 dimethylation, as reported before for *GFI1-36N* cells.[9,17] This explanation is consistent with other studies that have reported a correlation between the number of open chromatin states and susceptibility to DNA damage.[58] In summary, the presence of *GFI1-36N* in leukemic cells leads to higher chromatin accessibility and reduced HR- and MGMT-mediated DNA repair.

Targeting MGMT via temozolomide with tumors coopting mutations in the DNA damage repair gene was shown to achieve an exceptional response to cancer therapy.[59] Both HR-directed and MGMT-mediated DNA repair pathways have been targeted in different cancer entities using temozolomide and/or olaparib.[32,47,49,60-62] Temozolomide alone or in combination with olaparib significantly reduced the expansion of murine and human *GFI1-36N* leukemic cells in vitro and in vivo without affecting nonleukemic cells. Finally, use of another PARP inhibitor induced in an albeit small cohort a 75% rate of CRi among patients with heterozygous or homozygous *GFI1-36N*. PARP inhibitors and temozolomide in combination with, for example, cytotoxic therapy have well-manageable side effects, which could prove to be particularly beneficial for older patients with *GFI1-36N*–positive AML. Although temozolomide and olaparib can induce further mutations, which is also true for other chemotherapeutic approaches, PARP inhibitors and alkylating agents offer the possibility of selectively targeting *GFI1-36N* leukemic cells in potential future trials.

Acknowledgments

The authors thank the Core Facility Genomics of the University Muenster and Genomics and Transcriptomics Facility for RNA sequencing. Furthermore, the authors also thank the Imaging Center Essen and the Fluorescence Microscopy Facility Münster for guidance and providing the microscopes. The authors also thank Maria Eynck, Renata Köster, Dagmar Clemens, Hannelore Leuschke, and Claudia Dill for their technical assistance, and Klaus Lennartz and Thorsten König for their assistance with cell sorting. The authors thank the members of Proteomics and Signal Transduction Department at the Max Planck Institute for Biochemistry, particularly Igor Paron for his technical support. H.B. and A.K. acknowledge computational support from the OMICS compute cluster at the University of Lübeck.

The work was supported by the Deutsche Krebshilfe (70112392) and partially by the Jose Carreras Leukämie Stiftung (DJCLS 17R/2018), Deutsche Forschungsgemeinschaft (KH331/2-3), and the intramural funding of the faculty of Medicine at University Hospital of Muenster (Kha2/002/20). This study was supported by AstraZeneca and Merck Sharp & Dohme Corp, a subsidiary of Merck & Co Inc, Kenilworth, NJ, who are codeveloping olaparib. J. Vorwerk was supported by the Jürgen Manchot Foundation and the Medizinerkolleg Münster. A.K.J. and M.M. were supported by the Max Planck Society for the Advancement of Science and by the German Research Foundation (Gottfried Wilhelm Leibniz Prize). A.K.J. is supported by DFG Emmy Noether grant

Downloaded from http://ashpublications.net/blood/article-pdf/142/25/2175/2177539/blood_bld-2022-015752-main.pdf by guest on 03 May 2024

(JA3274/1-1). H.B. was supported by the Deutsche Forschungsgemeinschaft (German Research Foundation) under Germany's Excellence Strategy EXC 22167-390884018, partially funded by the Bundesministerium für Bildung und Forschung grant 01ZZ1804B (DIFUTURE) (A.M.N.B.).

Authorship

Contribution: D.F., J. Vorwerk, L.M., L.M.G., N.J., Y.A.-M., P.K.P., H.M.M.A., L.L., X.X., K.S., L.M.G., E.W., J.T., F.S., L.R., and A.K.J. performed experimental research; D.F., F.C.C., H.A., M.G., M.S., and D.K. genotyped human patient samples; D.F., J. Vorwerk, J.H., and F.N. took the fluorescence images; D.F., J.M.F., A.K., H.M., S.H., L.W., V.C., E.W., S.K.M., J.W.T., A.K.J., T.L., and C.K. performed data analysis, presentation, and interpretation; A.F. performed data analysis and edited the manuscript; C.R. provided samples, performed data analysis, and edited the manuscript; N.v.B. and G.L. provided funding and samples, analysed data, and edited the manuscript; A.M.N.B., R.A., and T.H. performed bioinformatics analyses; H.B., G.H., M.D., M.K., and J. Varghese supervised and supported bioinformatics analyses; R.R. provided essential mouse strains and performed the analysis of the mouse model; J.T. performed the immunostaining, the measurements and the evaluation of the O^6MeG assays; A.K.J., L.M., M.K., T.H., and J.M.F. performed mass spectrometry experiments, data analysis, and bioinformatics; A.K.J. and M.M. provided support and supervised the mass spectrometry experiments; V.C. and T.M. analyzed GFI1-binding sites in hematopoietic precursor cells; M.H., F.T., G.G., D.S., J.T., F.S., W.E.B., J.K., F.R., A.K., M.D., U.D., M.M., A.K.J., M.H., J. Vorwerk, H.C.R., and C.K. provided essential data or samples or research support; D.F., A.K.J., and C.K. designed the study and wrote the manuscript; S.C.N., B.O., and T.M. critically revised the article; and all authors read, provided critical comments, and approved the manuscript.

Conflict-of-interest disclosure: H.C.R. received consulting and lecture fees from AbbVie, AstraZeneca, Vertex, and Merck; received research funding from Gilead Pharmaceuticals; and is a cofounder of CDL Therapeutics GmbH. G.H. received consulting and lecture fees from Novartis, Incyte, and Jazz Pharmaceuticals. C.K. received funding from AstraZeneca for this project. E.W. received funding from Pfizer for conducting the clinical trial. The remaining authors declare no competing financial interests.

B.O. and U.D. are retired from University Hospital Essen, Essen, Germany.

ORCID profiles: P.K.P., 0000-0002-2605-4475; J.M.F., 0000-0001-8696-3817; M.K., 0000-0001-6866-0417; L.W., 0000-0002-4281-8017; H.M.M.A., 0000-0001-8298-4135; A.K., 0000-0003-0692-2105; H.B., 0000-0003-4763-4521; S.H., 0000-0003-2432-8898; L.L., 0000-0003-2156-1715; C.R., 0000-0002-3791-0548; D.K., 0000-0001-8750-5308; W.E.B., 0000-0002-3030-6567; M.D., 0000-0001-9740-0788; N.v.B., 0000-0001-9593-8947; A.M.N.B., 0000-0002-7972-7506; M.S., 0000-0002-5939-2251; S.K.M., 0000-0001-8333-6607; F.S., 0000-0003-0653-5332; M.M., 0000-0003-1292-4799; A.K.J., 0000-0002-3292-1117; C.K., 0000-0003-4655-6269.

Correspondence: Matthias Mann, Department of Proteomics and Signal Transduction, Max Planck Institute of Biochemistry, Am Klopferspitz 18, 82152 Martinsried, Germany; email: mmann@biochem.mpg.de; Ashok Kumar Jayavelu, Proteomics and Cancer Cell Signaling, Deutsches Krebsforschungszentrum, Im Neuenheimer Feld 280, 69120 Heidelberg, Germany; email: ak.jayavelu@dkfz-heidelberg.de; and Cyrus Khandanpour, Department of Hematology and Oncology, University Cancer Center Schleswig- Holstein, University Hospital of Schleswig-Holstein Campus Lübeck and University of Lübeck, Ratzeburger-Allee 160, 23564 Luebeck, Germany; email: cyrus.khandanpour@uksh.de.

Footnotes

Submitted 7 February 2022; accepted 24 July 2023; prepublished online on *Blood* First Edition 26 September 2023. https://doi.org/10.1182/blood.2022015752.

RNA-seq data are deposited in the Gene Expression Omnibus database (accession number GSE195955). Proteome data are deposited in the proteome repository (accession number PXD037433).

Other original data are available on request from the corresponding authors, Matthias Mann (mmann@biochem.mpg.de), Ashok Kumar Jayavelu (ak.jayavelu@dkfz-heidelberg.de), and and Cyrus Khandanpour (cyrus.khandanpour@uksh.de).

The online version of this article contains a data supplement.

The publication costs of this article were defrayed in part by page charge payment. Therefore, and solely to indicate this fact, this article is hereby marked "advertisement" in accordance with 18 USC section 1734.

REFERENCES

1. Hock H, Hamblen MJ, Rooke HM, et al. Gfi-1 restricts proliferation and preserves functional integrity of haematopoietic stem cells. *Nature*. 2004;431(7011):1002-1007.
2. Karsunky H, Zeng H, Schmidt T, et al. Inflammatory reactions and severe neutropenia in mice lacking the transcriptional repressor Gfi1. *Nat Genet*. 2002;30(3):295-300.
3. Thambyrajah R, Mazan M, Patel R, et al. GFI1 proteins orchestrate the emergence of haematopoietic stem cells through recruitment of LSD1. *Nat Cell Biol*. 2016;18(1):21-32.
4. Yucel R, Kosan C, Heyd F, Moroy T. Gfi1: green fluorescent protein knock-in mutant reveals differential expression and autoregulation of the growth factor independence 1 (Gfi1) gene during lymphocyte development. *J Biol Chem*. 2004;279(39):40906-40917.
5. Zeng H, Yücel R, Kosan C, Klein-Hitpass L, Möröy T. Transcription factor Gfi1 regulates self-renewal and engraftment of hematopoietic stem cells. *EMBO J*. 2004;23(20):4116-4125.
6. Khandanpour C, Thiede C, Valk PJ, et al. A variant allele of growth factor independence 1 (GFI1) is associated with acute myeloid leukemia. *Blood*. 2010;115(12):2462-2472.
7. Botezatu L, Michel LC, Makishima H, et al. GFI1(36N) as a therapeutic and prognostic marker for myelodysplastic syndrome. *Exp Hematol*. 2016;44(7):590-595.e1.
8. Khandanpour C, Eisfeld C, Nimmagadda SC, et al. Prevalence of the GFI1-36N SNP in multiple myeloma patients and its impact on the prognosis. *Front Oncol*. 2021;11:757664.
9. Botezatu L, Michel LC, Helness A, et al. Epigenetic therapy as a novel approach for GFI136N-associated murine/human AML. *Exp Hematol*. 2016;44(8):713-726.e14.
10. Phelan JD, Shroyer NF, Cook T, Gebelein B, Grimes HL. Gfi1-cells and circuits: unraveling transcriptional networks of development and disease. *Curr Opin Hematol*. 2010;17(4):300-307.
11. Saleque S, Kim J, Rooke HM, Orkin SH. Epigenetic regulation of hematopoietic differentiation by Gfi-1 and Gfi-1b is mediated by the cofactors CoREST and LSD1. *Mol Cell*. 2007;27(4):562-572.
12. McGhee L, Bryan J, Elliott L, et al. Gfi-1 attaches to the nuclear matrix, associates with ETO (MTG8) and histone deacetylase proteins, and represses transcription using a TSA-sensitive mechanism. *J Cell Biochem*. 2003;89(5):1005-1018.
13. Montoya-Durango DE, Velu CS, Kazanjian A, et al. Ajuba functions as a histone deacetylase-dependent co-repressor for autoregulation of the growth factor-independent-1 transcription factor. *J Biol Chem*. 2008;283(46):32056-32065.

Downloaded from http://ashpublications.net/blood/article-pdf/142/25/2175/2177539/blood_bld-2022-015752-main.pdf by guest on 03 May 2024

14. Horman SR, Velu CS, Chaubey A, et al. Gfi1 integrates progenitor versus granulocytic transcriptional programming. *Blood*. 2009; 113(22):5466-5475.

15. Duan Z, Horwitz M. Targets of the transcriptional repressor oncoprotein Gfi-1. *Proc Natl Acad Sci U S A*. 2003;100(10): 5932-5937.

16. Duan Z, Zarebski A, Montoya-Durango D, Grimes HL, Horwitz M. Gfi1 coordinates epigenetic repression of p21Cip/WAF1 by recruitment of histone lysine methyltransferase G9a and histone deacetylase 1. *Mol Cell Biol*. 2005;25(23): 10338-10351.

17. Khandanpour C, Krongold J, Schütte J, et al. The human GFI136N variant induces epigenetic changes at the Hoxa9 locus and accelerates K-RAS driven myeloproliferative disorder in mice. *Blood*. 2012;120(19): 4006-4017.

18. Vadnais C, Chen R, Fraszczak J, et al. GFI1 facilitates efficient DNA repair by regulating PRMT1 dependent methylation of MRE11 and 53BP1. *Nat Commun*. 2018;9(1):1418.

19. Schlenk RF, Dohner K, Krauter J, et al. Mutations and treatment outcome in cytogenetically normal acute myeloid leukemia. *N Engl J Med*. 2008;358(18): 1909-1918.

20. Schulz E, Lind K, Renner W, et al. The TP53 Pro72Arg SNP in de novo acute myeloid leukaemia - results of two cohort studies involving 215 patients and 3759 controls. *Br J Haematol*. 2018;181(1):148-151.

21. Stengel A, Shahswar R, Haferlach T, et al. Whole transcriptome sequencing detects a large number of novel fusion transcripts in patients with AML and MDS. *Blood Adv*. 2020;4(21):5393-5401.

22. Lin Y-W, Slape C, Zhang Z, Aplan PD. NUP98-HOXD13 transgenic mice develop a highly penetrant, severe myelodysplastic syndrome that progresses to acute leukemia. *Blood*. 2005;106(1):287-295.

23. Rad R, Rad L, Wang W, et al. PiggyBac transposon mutagenesis: a tool for cancer gene discovery in mice. *Science*. 2010; 330(6007):1104-1107.

24. Rad R, Rad L, Wang W, et al. A conditional piggyBac transposition system for genetic screening in mice identifies oncogenic networks in pancreatic cancer. *Nat Genet*. 2015;47(1):47-56.

25. Hönes JM, Thivakaran A, Botezatu L, et al. Enforced GFI1 expression impedes human and murine leukemic cell growth. *Sci Rep*. 2017;7(1):15720.

26. Kulak NA, Pichler G, Paron I, Nagaraj N, Mann M. Minimal, encapsulated proteomic-sample processing applied to copy-number estimation in eukaryotic cells. *Nat Methods*. 2014;11(3):319-324.

27. Tate JG, Bamford S, Jubb HC, et al. COSMIC: the catalogue of somatic mutations in cancer. *Nucleic Acids Res*. 2019;47(D1):D941-D947.

28. Ohba S, Mukherjee J, See WL, Pieper RO. Mutant IDH1-driven cellular transformation increases RAD51-mediated homologous recombination and temozolomide resistance. *Cancer Res*. 2014;74(17):4836-4844.

29. Chapman JR, Taylor MR, Boulton SJ. Playing the end game: DNA double-strand break repair pathway choice. *Mol Cell*. 2012;47(4): 497-510.

30. Ciccia A, Elledge SJ. The DNA damage response: making it safe to play with knives. *Mol Cell*. 2010;40(2):179-204.

31. Panier S, Boulton SJ. Double-strand break repair: 53BP1 comes into focus. *Nat Rev Mol Cell Biol*. 2014;15(1):7-18.

32. Cohen MH, Johnson JR, Pazdur R. Food and Drug Administration drug approval summary: temozolomide plus radiation therapy for the treatment of newly diagnosed glioblastoma multiforme. *Clin Cancer Res*. 2005;11(19 pt 1):6767-6771.

33. Goode DK, Obier N, Vijayabaskar MS, et al. Dynamic gene regulatory networks drive hematopoietic specification and differentiation. *Dev Cell*. 2016;36(5): 572-587.

34. Jayavelu AK, Wolf S, Buettner F, et al. The proteogenomic subtypes of acute myeloid leukemia. *Cancer Cell*. 2022;40(3):301-317. e12.

35. Hegi ME, Liu L, Herman JG, et al. Correlation of O6-methylguanine methyltransferase (MGMT) promoter methylation with clinical outcomes in glioblastoma and clinical strategies to modulate MGMT activity. *J Clin Oncol*. 2008;26(25):4189-4199.

36. Esteller M, Hamilton SR, Burger PC, Baylin SB, Herman JG. Inactivation of the DNA repair gene O6-methylguanine-DNA methyltransferase by promoter hypermethylation is a common event in primary human neoplasia. *Cancer Res*. 1999; 59(4):793-797.

37. Spooner CJ, Lesch J, Yan D, et al. Specification of type 2 innate lymphocytes by the transcriptional determinant Gfi1. *Nat Immunol*. 2013;14(12):1229-1236.

38. Moignard V, Macaulay IC, Swiers G, et al. Characterization of transcriptional networks in blood stem and progenitor cells using high-throughput single-cell gene expression analysis. *Nat Cell Biol*. 2013;15(4):363-372.

39. Weiler M, Blaes J, Pusch S, et al. mTOR target NDRG1 confers MGMT-dependent resistance to alkylating chemotherapy. *Proc Natl Acad Sci U S A*. 2014;111(1):409-414.

40. Erasimus H, Gobin M, Niclou S, Van Dyck E. DNA repair mechanisms and their clinical impact in glioblastoma. *Mutat Res Rev Mutat Res*. 2016;769:19-35.

41. Northcott PA, Lee C, Zichner T, et al. Enhancer hijacking activates GFI1 family oncogenes in medulloblastoma. *Nature*. 2014;511(7510):428-434.

42. Sun W, Guo J, McClellan D, et al. GFI1 cooperates with IKZF1/IKAROS to activate gene expression in T-cell acute lymphoblastic leukemia. *Mol Cancer Res*. 2022;20(4):501-514.

43. Spooner CJ, Cheng JX, Pujadas E, Laslo P, Singh H. A recurrent network involving the transcription factors PU.1 and Gfi1 orchestrates innate and adaptive immune cell fates. *Immunity*. 2009;31(4):576-586.

44. Grant CE, Bailey TL, Noble WS. FIMO: scanning for occurrences of a given motif. *Bioinformatics*. 2011;27(7):1017-1018.

45. Castro-Mondragon JA, Riudavets-Puig R, Rauluseviciute I, et al. JASPAR 2022: the 9th release of the open-access database of transcription factor binding profiles. *Nucleic Acids Res*. 2022;50(D1):D165-D173.

46. Zhang J, Stevens MF, Bradshaw TD. Temozolomide: mechanisms of action, repair and resistance. *Curr Mol Pharmacol*. 2012; 5(1):102-114.

47. Singh R, Mehrotra S, Gopalakrishnan M, et al. Population pharmacokinetics and exposure-response assessment of veliparib co-administered with temozolomide in patients with myeloid leukemias. *Cancer Chemother Pharmacol*. 2019;83(2):319-328.

48. Gojo I, Beumer JH, Pratz KW, et al. A phase 1 study of the PARP inhibitor veliparib in combination with temozolomide in acute myeloid leukemia. *Clin Cancer Res*. 2017; 23(3):697-706.

49. Farago AF, Yeap BY, Stanzione M, et al. Combination olaparib and temozolomide in relapsed small-cell lung cancer. *Cancer Discov*. 2019;9(10):1372-1387.

50. Khandanpour C, Phelan JD, Vassen L, et al. Growth factor independence 1 antagonizes a p53-induced DNA damage response pathway in lymphoblastic leukemia. *Cancer Cell*. 2013;23(2):200-214.

51. Khandanpour C, Moroy T. Growth factor independence 1 (Gfi1) as a regulator of p53 activity and a new therapeutical target for ALL. *Oncotarget*. 2013;4(3):374-375.

52. Dohner H, Wei AH, Appelbaum FR, et al. Diagnosis and management of AML in adults: 2022 recommendations from an international expert panel on behalf of the ELN. *Blood*. 2022;140(12):1345-1377.

53. Kiwerska K, Szyfter K. DNA repair in cancer initiation, progression, and therapy-a double-edged sword. *J Appl Genet*. 2019;60(3-4): 329-334.

54. Dietlein F, Thelen L, Reinhardt HC. Cancer-specific defects in DNA repair pathways as targets for personalized therapeutic approaches. *Trends Genet*. 2014;30(8): 326-339.

55. Alcalay M, Meani N, Gelmetti V, et al. Acute myeloid leukemia fusion proteins deregulate genes involved in stem cell maintenance and DNA repair. *J Clin Invest*. 2003;112(11): 1751-1761.

56. Bret C, Viziteu E, Kassambara A, Moreaux J. Identifying high-risk adult AML patients: epigenetic and genetic risk factors and their implications for therapy. *Expert Rev Hematol*. 2016;9(4):351-360.

Downloaded from http://ashpublications.net/blood/article-pdf/142/25/2175/2177539/blood_bld-2022-015752-main.pdf by guest on 03 May 2024

57. Helness A, Fraszczak J, Joly-Beauparlant C, et al. GFI1 tethers the NuRD complex to open and transcriptionally active chromatin in myeloid progenitors. *Commun Biol*. 2021; 4(1):1356.

58. Nair N, Shoaib M, Sørensen CS. Chromatin dynamics in genome stability: roles in suppressing endogenous DNA damage and facilitating DNA repair. *Int J Mol Sci*. 2017; 18(7):1486.

59. Wheeler DA, Takebe N, Hinoue T, et al. Molecular features of cancers exhibiting exceptional responses to treatment. *Cancer Cell*. 2021;39(1):38-53.e7.

60. Hou WH, Chen SH, Yu X. Poly-ADP ribosylation in DNA damage response and cancer therapy. *Mutat Res Rev Mutat Res*. 2019;780:82-91.

61. Silber JR, Bobola MS, Blank A, Chamberlain MC. O(6)-methylguanine-DNA methyltransferase in glioma therapy: promise and problems. *Biochim Biophys Acta*. 2012; 1826(1):71-82.

62. Kontandreopoulou CN, Diamantopoulos PT, Tiblalexi D, Giannakopoulou N, Viniou NA. PARP1 as a therapeutic target in acute myeloid leukemia and myelodysplastic syndrome. *Blood Adv*. 2021;5(22):4794-4805.

© 2023 by The American Society of Hematology. Licensed under Creative Commons Attribution-NonCommercial-NoDerivatives 4.0 International (CC BY-NC-ND 4.0), permitting only noncommercial, nonderivative use with attribution. All other rights reserved.

Downloaded from http://ashpublications.net/blood/article-pdf/142/25/2175/2177539/blood_bld-2022-015752-main.pdf by guest on 03 May 2024